Lethal Borna disease virus 1 (BoDV-1) infections of humans and animals – in-depth molecular epidemiology and phylogeography

Dennis Rubbenstroth (✉ Dennis.Rubbenstroth@fli.de)
Friedrich-Loeffler-Institut https://orcid.org/0000-0002-8209-6274

Arnt Ebinger
Friedrich-Loeffler-Institut

Pauline Santos
Friedrich-Loeffler-Institut

Florian Pfaff
Friedrich-Loeffler-Institut https://orcid.org/0000-0003-0178-6183

Ralf Dürrwald
German National Influenza Center https://orcid.org/0000-0002-3432-0438

Jolanta Kolodziejek
University of Veterinary Medicine https://orcid.org/0000-0001-5736-3644

Kore Schlottau
Institute of Diagnostic Virology, Friedrich-Loeffler-Institut, Federal Research Institute of animal health
https://orcid.org/0000-0002-3999-0393

Viktoria Ruf
Ludwig-Maximilians-Universität München

Friederike Liesche-Starnecker
University of Augsburg

Armin Ensser
University Hospital Erlangen

Klaus Korn
Friedrich-Alexander Universität Erlangen-Nürnberg

Reiner Ulrich
Institute of Veterinary Pathology, Leipzig University

Jenny Fürstenau
Freie Universität Berlin

Kaspar Matiasek
Section of Clinical & Comparative Neuropathology, Centre for Clinical Veterinary Medicine, LMU Munich
https://orcid.org/0000-0001-5021-3280

Florian Hansmann

Leipzig University

Torsten Seuberlich

University of Bern

Daniel Nobach

Justus-Liebig-University Giessen

Matthias Müller

Bavarian Health and Food Safety Authority

Antonie Neubauer-Juric

Bavarian Health and Food Safety Authority

Marcel Suchowski

Bavarian Health and Food Safety Authority

Markus Bauswein

Regensburg University Hospital

Hans-Helmut Niller

Regensburg University

Barbara Schmidt

Regensburg University Hospital

Dennis Tappe

Bernhard Nocht-Institute for Tropical Medicine

Daniel Cadar

Bernhard Nocht-Institute for Tropical Medicine

Timo Homeier-Bachmann

Friedrich-Loeffler-Institute Federal Research Institute for Animal Health https://orcid.org/0000-0002-8135-3814

Viola Haring

Friedrich-Loeffler-Institut https://orcid.org/0009-0007-7595-8239

Kirsten Pörtner

Robert Koch Institute

Christina Frank

Robert Koch Institute

Lars Mundhenk

Freie Universität Berlin https://orcid.org/0000-0002-9033-9360

Bernd Hoffmann

Institute of Diagnostic Virology, Friedrich-Loeffler-Institut, Federal Research Institute of animal health https://orcid.org/0000-0001-5358-6445

Jochen Herms

Center for Neuropathology, Ludwig-Maximilians-University https://orcid.org/0000-0002-6201-1042

Wolfgang Baumgärtner

Department of Pathology, University of Veterinary Medicine, Foundation https://orcid.org/0000-0001-8151-5644

Norbert Nowotny
University of Veterinary Medicine, Austria https://orcid.org/0000-0002-3548-571X

Jürgen Schlegel
Technical University Munich

Rainer G. Ulrich
Friedrich Löffler Institut https://orcid.org/0000-0002-5620-1528

Martin Beer
Friedrich-Loeffler-Institute https://orcid.org/0000-0002-0598-5254

Article

Keywords:

Posted Date: November 29th, 2023

DOI: https://doi.org/10.21203/rs.3.rs-3640627/v1

Additional Declarations: There is **NO** Competing Interest.

Lethal Borna disease virus 1 (BoDV-1) infections of humans and animals – in-depth molecular epidemiology and phylogeography

Arnt Ebinger[1,†], Pauline D. Santos[1], Florian Pfaff[1], Ralf Dürrwald[2], Jolanta Kolodziejek[3], Kore Schlottau[1], Viktoria Ruf[4], Friederike Liesche-Starnecker[5,6], Armin Ensser[7], Klaus Korn[7], Reiner Ulrich[8], Jenny Fürstenau[9], Kaspar Matiasek[10], Florian Hansmann[8,11], Torsten Seuberlich[12], Daniel Nobach[13,14], Matthias Müller[15], Antonie Neubauer-Juric[16], Marcel Suchowski[8,16], Markus Bauswein[17], Hans-Helmut Niller[18], Barbara Schmidt[17], Dennis Tappe[19], Daniel Cadar[19], Timo Homeier-Bachmann[20], Viola C. Haring[21], Kirsten Pörtner[22], Christina Frank[22], Lars Mundhenk[9], Bernd Hoffmann[1], Jochen Herms[4], Wolfgang Baumgärtner[11], Norbert Nowotny[3,23], Jürgen Schlegel[5], Rainer G. Ulrich[22], Martin Beer[1], Dennis Rubbenstroth[1]*

[1] Institute of Diagnostic Virology, Friedrich-Loeffler-Institut, Greifswald-Insel Riems, Germany

[2] Robert Koch Institute, Department of Infectious Diseases, Unit 17 Influenza and Other Respiratory Viruses, National Reference Centre for Influenza, Berlin, Germany

[3] Institute of Virology, University of Veterinary Medicine Vienna, Vienna, Austria

[4] Center for Neuropathology and Prion Research, Faculty of Medicine, Ludwig-Maximilians Universität München, Munich, Germany

[5] Department of Neuropathology, School of Medicine, Institute of Pathology, Technical University Munich, Munich, Germany

[6] Pathology, Medical Faculty, University of Augsburg, Augsburg, Germany

[7] Institute of Virology, University Hospital Erlangen, Friedrich-Alexander Universität Erlangen-Nürnberg (FAU), Erlangen, Germany

[8] Institute of Veterinary Pathology, Faculty of Veterinary Medicine, Leipzig University, Leipzig, Germany

[9] Institute of Veterinary Pathology, Freie Universität Berlin, Berlin, Germany

[10] Section of Clinical & Comparative Neuropathology, Centre for Clinical Veterinary Medicine, Ludwig-Maximilians-Universität München, Munich, Germany

[11] Department of Pathology, University of Veterinary Medicine Hannover, Hannover, Germany

[12] Division of Neurological Sciences, Vetsuisse Faculty, University of Bern, Bern, Switzerland

[13] Institute of Veterinary Pathology, Justus-Liebig-University Giessen, Giessen, Germany

[14] Chemical and Veterinary Analysis Agency Stuttgart (CVUAS), Fellbach, Germany

[15] Bavarian Health and Food Safety Authority, Erlangen, Germany

[16] Bavarian Health and Food Safety Authority, Oberschleißheim, Germany

[17] Institute of Clinical Microbiology and Hygiene, Regensburg University Hospital, Regensburg, Germany

[18] Institute for Medical Microbiology, Regensburg University, Regensburg, Germany

[19] Bernhard Nocht-Institute for Tropical Medicine, Hamburg, Germany

[20] Institute of Epidemiology, Friedrich-Loeffler-Institut, Greifswald-Insel Riems, Germany

[21] Institute of Novel and Emerging Infectious Diseases, Friedrich-Loeffler-Institut, Greifswald-Insel Riems, Germany

[22] Robert Koch Institute, Department of Infectious Disease Epidemiology, Berlin, Germany

[23] Department of Basic Medical Sciences, College of Medicine, Mohammed Bin Rashid University of Medicine and Health Sciences, Dubai, United Arab Emirates

[†]Current address: University Medicine Greifswald, Fleischmannstraße 8, Greifswald, Germany

* Corresponding author:

Dennis Rubbenstroth, Friedrich-Loeffler-Institut, Institute of Diagnostic Virology, Greifswald-Insel Riems, Germany, Email: Dennis.Rubbenstroth@fli.de

Abstract

Borna disease virus 1 (BoDV-1) is the causative agent of Borna disease, a progressive and mostly fatal neurologic disorder of domestic mammals and humans, resulting from spill-over infection from its natural reservoir host, the bicolored white-toothed shrew (*Crocidura leucodon*). The known BoDV-1 endemic area is remarkably restricted to parts of Germany, Austria, Switzerland and the Principality of Liechtenstein.

To gain comprehensive data on the occurrence of BoDV-1, we analysed diagnostic material from suspected fatal BoDV-1-induced encephalitis cases in domestic mammals and humans. BoDV-1 infection was confirmed by RT-qPCR in 207 of 231 domestic mammals (89.6%), 28 of 29 humans (96.6%) and seven shrews, mainly within the known endemic area. By reporting multiple unpublished cases, this study raises the number of published laboratory-confirmed human BoDV-1 infections to 46 and provides a first comprehensive summary.

Generation of 136 new complete or partial BoDV-1 genome sequences from animals and humans facilitated an in-depth phylogeographic analysis. Consistent with the low mobility of its reservoir host, BoDV-1 sequences showed a remarkable geographic association, with individual phylogenetic clades occupying distinct and barely overlapping dispersal areas. The closest genetic relatives of most human-derived BoDV-1 sequences were located at distances of less than 40 km from the patient's residence, indicating that spill-over transmission from the natural reservoir usually occurs in the region of the patient´s residence.

In summary, the novel and extended phylogeographic data allow for the definition of risk areas for zoonotic BoDV-1 transmission and facilitate the assessment of geographical sources for individual infection events.

Introduction

Borna disease virus 1 (BoDV-1, species *Orthobornavirus bornaense*, family *Bornaviridae*) is the causative agent of Borna disease, a severe and often fatal neurologic disease of various domestic mammals, particularly horses, sheep, and New World camelids [1, 2, 3, 4, 5]. Recently, the virus received increased attention following confirmation of fatal BoDV-1-induced encephalitis in humans [6, 7, 8, 9, 10, 11, 12, 13, 14, 15, 16, 17, 18]. In domestic mammals and humans, BoDV-1 establishes a persistent and strictly neurotropic infection mainly of the central nervous system, with so far no evidence of shedding of infectious virus. The infection usually results in non-purulent encephalomyelitis due to T lymphocyte-mediated immunopathology with a high case fatality rate [1, 7, 9, 19, 20]. The incubation period is presumably highly variable and assumed to range from several weeks to a few months in most cases [8, 21, 22]. Affected individuals usually develop fever accompanied by headaches in humans, followed by a broad range of behavioural and neurologic disorders, including apathy, compulsive movements, seizures, ataxia or blindness. In most cases, the disease progresses to coma and death within days to months [1, 2, 6, 7, 10, 17, 23, 24]. Several compounds have been identified to possess antiviral activity against orthobornaviruses in cell culture but no therapeutic regime for animals or humans has been established yet [25, 26, 27, 28], though in some human cases intensive treatment attempts were made [15][15]. As licensed vaccines against BoDV-1 are likewise not available [29], prophylactic measures are limited to reducing exposure to the BoDV-1 reservoir.

The only known natural reservoir host of BoDV-1 is the bicolored white-toothed shrew (*Crocidura leucodon*), in which BoDV-1 is not strictly neurotropic but also infects epithelial cells in various organs, thereby allowing for shedding of infectious virus via saliva, faeces, urine, and skin scales [4, 30, 31, 32, 33]. However, the routes of BoDV-1 transmission within shrew populations as well as for spill-over to domestic mammals and humans remain largely unknown [1, 17, 33, 34]. The known distribution range of bicolored white-toothed shrews covers large parts of the temperate zone of Europe and Western Asia, extending from the Atlantic ocean to the Caspian Sea [35, 36]. Nevertheless, BoDV-1 appears to be prevalent only in comparably limited regions covering parts of Eastern and Southern Germany, Austria, Switzerland and the Principality of Liechtenstein, based on the occurrence of BoDV-1 infection in spill-

over hosts [4, 7, 24, 32, 37]. Previous work had demonstrated BoDV-1 sequences to constitute four separate phylogenetic clusters (designated 1 to 4) with two subclusters (1A and 1B), which appear to be associated with different regions within the endemic area [4, 7, 8, 11, 12, 24, 32, 34, 37, 38, 39, 40].

The aim of this study was to provide an in-depth analysis of the molecular epidemiology and phylogeography of BoDV-1, in particular its spatial distribution in Germany and neighbouring countries, and to assess geographic risk areas for potential spill-over transmission to domestic animals and humans. As the available data on the occurrence of BoDV-1 in shrew populations are highly fragmentary and strongly dependent on the activities of a small number of research groups [4, 24, 30, 31, 32, 33, 41], we collected material from archived and current cases of Borna disease in domestic mammals, serving as indicators for the presence of the virus. Additional diagnostic samples were obtained from BoDV-1-infected human patients and bicolored white-toothed shrews. BoDV-1 sequences were generated from this material and used for phylogeographic analysis including also sequence data derived from public databases.

Material and Methods

Acquisition of sample material

Veterinary pathologists and federal and private veterinary diagnostic laboratories in Germany, Switzerland and Austria were informed about the study through presentations at scientific meetings, publications in national specialist journals, via mailing lists of expert societies and by direct contact. In total, 20 institutions provided fresh-frozen or formalin-fixed paraffin-embedded (FFPE) brain tissue or cerebrospinal fluid (CSF) from 231 archived or current suspected BoDV-1 infections in domestic mammals (including few zoo animals; Table 1; Extended Data Table 1). Some, but not all, of these infections had already been diagnosed by the submitting diagnostic laboratories. In addition, brain samples from 29 archived or recent human BoDV-1 encephalitis cases were obtained from diagnostic centres and pathologists in Germany. These cases included unpublished cases as well as previously published cases without available BoDV-1 sequence [7, 9, 14, 16, 17, 18] (Table 1). In addition, samples from seven BoDV-1-positive bicolored white-toothed shrews were obtained from an ongoing large-scale small mammal screening study (Haring et al., manuscript in preparation; Table 1). Furthermore, an original vaccine vial containing the historic BoDV-1 live vaccine strain 'Dessau', herein referred to as 'DessauVac' (batch 193 02 90; kindly provided by Sven Springer, IDT Biologika, now Ceva Santé Animale, Dessau-Rosslau, Germany), and the cell culture isolate H24 [38] were included for sequence analysis. In addition, the horse-derived cell culture isolates H640 and H3053 [37] were kindly provided for resequencing by Sybille Herzog (Gießen, Germany).

Acquisition of sample metadata

In order to facilitate spatio-temporal analyses, detailed metadata were requested from the submitters, including geographic location (postal code) and date of sampling, which was usually the date of death. Age, sex and date of hospital admission were recorded additionally for human cases. For animal cases, the accuracy of the geographic location was non-hierarchically categorized as follows: (1) the location of the animal husbandry is known, (2) the address of the owner is known, but the location of the husbandry is unknown and may be different, (3) only the submitting veterinary practice/clinic is

known, (4) only the administrative district of origin is known, (5) no information on the accuracy of the location is available.

In addition to the samples analysed in this study, previously published BoDV-1 sequences available via GenBank were included in the phylogeographic analysis (Table 1). The metadata described above (location, accuracy of location, host species, date of death or sampling) were assembled also for these cases, based on the available literature [4,6,7,9,10,11,12,13,15,21,24,32,37,38,39,42]. Missing data were completed by contacting the authors and/or the initial submitters, if possible.

The species of the seven analysed yellow-necked field mice had been confirmed by sequence analysis of the cytochrome B gene [43].

Extraction of total RNA

Fresh-frozen samples were mechanically disrupted in 1 ml TRIzol reagent (Life Technologies, Darmstadt, Germany) by using the TissueLyser II (Qiagen, Hilden, Germany), according to the manufacturers' instructions. After the addition of 200 µl chloroform and a centrifugation step (14,000 x *g*, 10 min, 4°C), the aqueous phase was collected and added to 250 µl isopropanol. Total RNA was extracted using the silica bead-based NucleoMagVet kit (Macherey & Nagel, Düren, Germany) with the KingFisher™ Flex Purification System (Thermo Fisher Scientific, Waltham, MA, USA) according to the manufacturers' instructions.

Additional RNA extraction from fresh-frozen samples selected for high-throughput sequencing (HTS) was performed according to Wylezich et al. [44]. Briefly, the tissue was rapidly frozen in liquid nitrogen and subsequently pulverized using the Covaris cryoPREP (Covaris, Brighton, UK). The resulting powdered tissue was then dissolved in pre-warmed 1 ml lysis buffer AL (Qiagen). RNA was extracted using the RNAdvance tissue kit (Beckman Coulter, Germany), including a DNase I (Qiagen) digestion step, in combination with a KingFisher Flex purification system (Thermo Fisher Scientific, Germany), according to the manufacturers' instructions. Total RNA was eluted in 100 µl nuclease-free water.

Total RNA from FFPE brain tissues was extracted as described previously [45]. Briefly, two FFPE sections of <10 µm thickness underwent deparaffinisation and proteinase K digestion employing the Covaris

truXTRAC FFPE total NA kit before RNA extraction, according to the manufacturer's instructions, resulting in 100 µl supernatant. To prevent the transfer of paraffin residues, formalin de-crosslinking was carried out using 85 µl of the supernatant in a clean 1.5 ml reaction tub (80 °C, 30 min, thermomixer). Subsequently, 175 µl of B1 Buffer from the Covaris kit and 250 µl of 65% isopropanol were added, mixed, and briefly centrifuged. Subsequently, RNA extraction was performed using the Agencourt RNAdvance Tissue Kit, as described above.

Detection of BoDV-1 RNA by RT-qPCR

BoDV-1 RNA was detected using two BoDV-1-specific RT-qPCR assays (Mix-1 & Mix-6) detecting phosphoprotein (P) and matrix protein (M) gene RNA, respectively (Extended Data Table 2), as described in detail elsewhere [8]. Exogenously supplemented, *in vitro*-transcribed RNA of the enhanced green fluorescence protein (eGFP) gene or host-derived beta-actin RNA were amplified as extraction control or RNA quality control, respectively, following previously described protocols [46, 47] (Extended Data Table 2).

High-throughput sequencing

HTS was performed for 114 selected BoDV-1 cases, including the cell culture isolates H24 and DessauVac (Table 1). Selection criteria for animal samples included spatial proximity to known human BoDV-1 cases or the occurrence in regions from which no or only few BoDV-1 sequences were available. If more than one case was available from a particular location, samples with higher predicted ratios of BoDV-1 RNA (indicated by lower RT-qPCR cycle of quantification [Cq] values) versus total RNA concentration were selected [48]. Libraries with an average DNA fragment size of 500 base pairs (bp) were prepared from fresh-frozen BoDV-1-positive brain samples with sufficient RNA quality following the procedure described by Wylezich et al. [44] with modifications by Szillat et al. [49]. Modified library preparation protocols were used for FFPE-samples as well as for fresh-frozen samples with lower RNA quality, resulting in a mean DNA fragment size of 200 bp [7]. Library quantification was carried out with the QIAseq Library Quant Assay Kit (Qiagen). Sequencing was performed using an Ion Torrent S5 XL instrument (Thermo Fisher Scientific). Libraries of 500 bp DNA fragment size were sequenced in 400

bp runs using Ion 530 chips, while libraries of 200 bp DNA fragment size were sequenced in 200 bp runs using Ion 540 or Ion 550 chips on an Ion S5 XL instrument.

HTS datasets were adapter- and quality-trimmed using the default settings of the 454 software suite (v3.0; Roche) before BoDV-1 reads were identified and extracted by mapping to the BoDV-1 reference sequence NC_001607. Duplicate BoDV-1 reads caused by library amplification were then removed using the SeqKit tool version 0.15.0 [50]. Mapping to the reference sequence was repeated for the remaining BoDV-1 reads. In parallel, the remaining BoDV-1 reads were *de novo* assembled using the 454 software suite and SPAdes v3.13.1 [51]. The accuracy of the resulting contigs was checked by comparing the consensus sequences generated by both approaches with each other and by sequence annotation as described below. Discrepancies were checked by reviewing the raw data from mapping and assembly, followed by manual sequence curation.

BoDV-1 target enrichment by hybridisation-based capture technology.

Enrichment of BoDV-1 specific library DNA fragments was performed for 16 selected samples for which insufficient BoDV-1 sequence information had been obtained by standard HTS (Table 1). For this purpose, an RNA bait set was designed for sequences representing all known members of the family *Bornaviridae* [5], resulting in 17,858 non-redundant specific RNA baits and providing a three-fold genome coverage with a length of 80 nucleotides (nt) per probe (myBaits® kit with 1–20K unique baits; Arbor Bioscience, Ann Arbor, MI, USA). The procedure was performed according to the manufacturer's instructions with minor modifications. Briefly, 7 µl of each DNA library were combined with the blocking reagent mix of the kit. After denaturation, 20 µl of a pre-warmed hybridisation mix, including the baits, was added. One volume of mineral oil was used to seal the reaction mix before incubation for 24 h at 65°C and shaking at 550 rpm in a thermomixer. The aqueous phase was then transferred to a low-binding tube and purified using the binding beads from the myBaits® kit. The enriched target library DNA was finally eluted in 35 µl of 10 mM Tris-HCl, 0.05% Tween-20 solution (pH 8.0-8.5) and amplified in duplicates (16 µl DNA each) using the GeneRead DNA Library L amplification Kit (Qiagen) with 10 cycles (denaturation: 2 min at 98°C; amplification for 10 cycles: 20 sec at 98°C, 30 sec 60°C,

and 30 sec at 72°C; final elongation: 1 min at 72°C). Subsequently, both duplicates were pooled and purified twice by adding 0.65 or 1.2 volumes of Agencourt AMPure XP Beads (Beckman Coulter) for 500 bp or 200 bp libraries, respectively. Enriched libraries were eluted in 30 µl buffer EB (Qiagen). Quality control and quantification of the eluted libraries as well as HTS were performed as described above.

Sanger sequencing

Partial BoDV-1 genome sequences were generated by Sanger sequencing for 43 BoDV-1-positive fresh-frozen brain samples (Table 1), following previously described procedures [24]. Briefly, a 2,272-nucleotide (nt) long sequence representing BoDV-1 genome positions 20 to 2,291 (spanning the nucleoprotein [N], accessory protein [X], P and partial M genes) was determined by sequencing two overlapping PCR products using BoDV-1-specific primers (Extended Data Table 2). The final consensus sequence was generated by assembly of the overlapping raw sequences after trimming of primer-derived sequence ends and manual quality control.

Sanger sequencing was also used to fill gaps or confirm not sufficiently reliable positions in sequences generated by HTS. For this purpose, BoDV-1-specific primer pairs were selected to generate amplicons of approximately 120 to 180 bp length to cover the respective sequence regions. Primer sequences are available upon request.

Sequence annotation and database submission

BoDV-1 sequences of sufficient length were generated from 136 of 157 selected individuals, including 102 domestic mammals, 25 humans, all seven bicolored white-toothed shrews as well as the laboratory isolates DessauVac and H24 (Table 1). These sequences included 54 complete coding genomes and 82 sequences covering at least the N-X/P genes (Table 1).

Open reading frames (ORFs) were identified by ORF Finder (implemented in Geneious Prime® 2021.0.1) and verified by sequence alignment to the reference sequence. All sequences generated in

this study are available in the INSDC databases under accession numbers OR203629, OR203630, OR468838 to OR468971.

Two previously published isolates (H640 and H3053) were re-analysed, because it was suspected that they may have been interchanged in the original study [37]. As the re-analysis of the original isolates confirmed this suspicion, the corresponding GenBank entries have now been corrected (accession numbers AY374523.2 and AY374537.2).

Phylogenetic analysis

Phylogenetic analysis of sequences generated in this study was performed together with those publicly available BoDV-1 sequences, which covered at least the N-X/P genes and for which sufficient metadata are available. The used public sequences originated from 55 domestic mammals, 16 human cases, 36 shrews and three laboratory strains isolated from domestic mammals (Table 1). Duplicate sequences originating from the same individual as well as sequences previously identified as laboratory contaminants were excluded from the analysis [7, 38, 39].

Maximum likelihood (ML) trees were constructed individually for 90 complete-coding sequences of BoDV-1 genomes and 246 sequences spanning the N-X/P genes (1,824 nt, corresponding to genome positions 54 to 1,877). For these analyses, the BoDV-2 No/98 sequence (AJ311524) was used as an outgroup. After sequence alignment using MUSCLE (version 3.8.425) [52], the IQ-TREE software (version 2.2.2.6) [53] was used for phylogenetic reconstruction with automatic model selection (SYM+G4 for complete genomes and GTR+F+I+G4 for N-X/P genes) [54]. Branch support was assessed using SH-aLRT and ultrafast bootstrap tests, with 100,000 replicates for each test [55, 56]. Nodes were extracted for better visualization using the ggtree R package [57] in R Studio [58] with R v4.0.2 [59]. Heatmap analysis of the genetic cluster similarities was performed using the pheatmap R-package [60].

Temporal and spatial correlation analysis

Root-to-tip distances and pairwise patristic distances (as nt substitutions per position) were inferred from the ML tree of 247 N-X/P sequences (incl. the BoDV-2 sequence). Temporal correlations were

tested by linear regression analysis of root-to-tip distances against year of sampling [61]. Sequences originating from laboratory strains were excluded from the analysis.

Isolation by distance (IBD) analysis was performed, testing the correlation of pairwise patristic distances and geographic distances for all BoDV-1 sequences with available location (n=238) as well as within the individual BoDV-1 clusters and subclusters. IBD matrix correlations were tested in R using the "mantel" function of the "vegan" package (Spearman's rho statistic and 9999 permutations).

Determination of BoDV-1 endemic areas

Geospatial data analysis and modelling was performed in R Studio with the packages rnaturalearth [62] and ggplot2 [63]. Non-parametric kernel density estimation (KDE) was used to visualize spatial distribution patterns of mapped BoDV-1 cases. KDE was performed independently for each phylogenetic cluster or subcluster as well as for sequences of all clusters and subclusters combined. BoDV-1 sequences identified as phylogeographic outliers by using the outlier definition described in detail in the results section (presence of no other BoDV-1 N-X/P sequence with ≥98.6% nt identity within a distance of ≤37.9 km) were excluded from the KDE.

The two-dimensional KDE, implemented in ggplot as the "stat_density_2d" function [64], was used with a polygon as the bounding box of estimated endemic regions. To smoothen the polygon, n=100 grid points were defined in each direction. A low bandwidth (h) was set empirically for both approaches in order to minimize the extent of the estimated areas beyond the confirmed cases (subcluster 1A: 1; subcluster 1B: 0.5; cluster 2: 0.6; cluster 3: 0.75; cluster 4: 0.65; combination of all clusters: 1.0).

Results

RT-qPCR confirmation of BoDV-1 infections in domestic mammals, humans and shrews

Veterinary and human pathologists and diagnostic laboratories submitted fresh-frozen or FFPE samples from 231 suspected BoDV-1 infections in domestic mammals, 29 humans and seven BoDV-1-positive shrews. The animals originated mainly from the known endemic regions of Germany (Bavaria, BY; Saxony-Anhalt, ST; Saxony, SN; Brandenburg, BB), Switzerland (Grisons, GR), the Principality of Liechtenstein and Austria (Vorarlberg, VA), with few exceptions originating from regions in Germany and Switzerland not previously known to be endemic for BoDV-1 (Figure 1A). RT-qPCR confirmed the BoDV-1 infection for 207 out of 231 domestic mammals (89.6%) and all analysed shrews. Of the 29 human cases analysed in this study, 28 (96.6%) could be confirmed by RT-qPCR. RT-qPCR and HTS remained negative for FFPE brain sections from a previously published case from Lower Saxony (NI) in 1992 [13], possibly due to low RNA quality resulting from long-term storage of the material.

The M gene-specific RT-qPCR BoDV-1 Mix-6 yielded significantly lower Cq values for FFPE material than the P gene-specific BoDV-1 Mix-1 (P<0.0001; paired Student´s t-test), whereas Mix-1 achieved significantly lower Cq values for fresh-frozen samples (P<0.0001; Extended Data Figure 1). The apparently higher sensitivity of Mix-6 for FFPE-derived RNA, as compared to Mix-1, is presumably due to its shorter amplicon (75 vs. 162 bp), allowing for a more efficient detection of highly degraded RNA.

BoDV-1 infections in domestic mammals and humans

Samples from most of the 207 confirmed BoDV-1 infections in domestic mammals were collected between 2000 and 2023, but individual cases dated back as far as 1964 (Extended Data Figure 2A and 2B). The seasonal pattern of Borna disease in domestic mammals was analysed for all RT-qPCR-confirmed cases together with all previously published cases included in this study with available information on month of death (Table 1). Death of BoDV-1-infected animals peaked in May and June, whereas the lowest numbers were observed during September to November (Extended Data Figure 3A).

This study raises the number of published laboratory-confirmed human BoDV-1 infections to 46 (Table 1), following the case definition of Eisermann et al. [11], which requires direct virus from the patient. Twenty-eight cases were confirmed by RT-qPCR during this study (including previously published cases without BoDV-1 sequence; [7, 9, 14, 16, 17, 18, 65, 66, 67]). BoDV-1 sequences were available from public databases for further 16 previously published human cases (Table 1) [6, 7, 8, 10, 11, 12, 13, 15]. Despite the lack of direct virus detection, the donor and the surviving liver recipient of a previously published solid organ transplant cluster were likewise regarded as confirmed cases due to their seroconversion and their unequivocal link to the confirmed BoDV-1 infections in both kidney recipients [8].

The metadata assembled for all 46 patients (20 females and 26 males) revealed a diagnosis of fulminant encephalitis for 45 patients, with a fatal outcome in 44 of the encephalitic patients (97.8%). The only exceptions from these characteristics were the transplant donor and the liver recipient of the previously published solid organ transplant cluster. While the donor had died of an unknown cause without brain histopathology being performed, the liver recipient survived the acute encephalitis with severe sequelae [8]. The age of the patients ranged from 7 to 79 years (median 53.5 years; Extended Data Figure 4A). The first of these confirmed cases occurred in 1996 and had been diagnosed retrospectively [10]. Six patients died in 2016, representing the highest number of confirmed non-transplant-derived cases per year (Extended Data Figure 2C). The highest number of deaths was recorded in November (Extended Data Figure 3B), while the highest number of hospitalizations was reported in May (Extended Data Figure 3C). The median time from hospital admission to death was 29 days (range: 4 to 274 days; Extended Data Figure 4B).

Phylogenetic analysis identifies a novel BoDV-1 cluster 5

During this study, BoDV-1 sequences covering the complete coding region of the genome (n=54) or at least the N and X/P genes (n=82) were successfully generated from 136 individuals, including 102 domestic mammals, 25 humans, all seven shrews and both laboratory strains (Table 1). Sequencing attempts failed or yielded only short sequence fragments for 18 additional domestic mammals and

three human cases, mainly due to low viral loads and/or insufficient RNA quality in FFPE and CSF samples.

Including additional BoDV-1 sequences from public databases, two ML trees were constructed for 90 complete coding BoDV-1 genomes (Figure 2) or 246 N-X/P sequences (Figure 3A, Extended Data Figure 5). Both trees supported the previously published clusters 2 to 4 and subclusters 1A and 1B with high statistical support (SH-aLRT ≥80% and ultrafast bootstrap ≥95%). The sequences from two human cases analysed in this study did not fall into any of the previously described clusters, but formed a separate cluster 5 basal to them (Figures 2 and 3A; Extended Data Figure 5).

To provide a more objectifiable basis for BoDV-1 cluster designation, we performed further analyses based on pairwise nt sequence identities of complete coding genomes (Extended Data Figure 6). Sequences belonging to the same cluster shared at least 96.0% pairwise nt identity, whereas sequences of different clusters were only up to 95.7% identical. Cluster 1 sequences shared 96.0 to 96.4% nt identity between subclusters 1A and 1B and at least 96.9% within each of the two subclusters, thus providing objectifiable demarcation criteria for cluster and subcluster assignment of complete coding genome sequences (Extended Data Figure 6). In agreement with these values, the two sequences of the novel cluster 5 possessed 99.0% nt identity with each other, but only 93.8 to 95.1% nt identity with any other BoDV-1 sequence, supporting their affiliation to a separate cluster.

Temporal and spatial relationships and host-association within BoDV-1 clusters

In agreement with the well-known genetic stability of orthobornaviruses [37, 39, 40], we observed pairs of nearly identical BoDV-1 sequences that were detected many years or even several decades apart from each other (Figure 2; Extended Data Figure 5). This observation was further confirmed by linear regression analysis of the ML tree root-to-tip divergence of BoDV-1 sequences over the past 43 years, which demonstrated the year of sampling to have no significant effect on the genetic divergence of the phylogenetic clusters and subclusters (R^2 = 0.0057 to 0.0570; P>0.05; Extended Data Figure 7).

Furthermore, the phylogenetic analysis did not reveal host-specific clades. With the exception of the novel cluster 5, all clusters and subclusters were composed of closely related sequences derived from

shrews and domestic mammals. Human sequences were identified in all clusters and subclusters except for subcluster 1B (Figures 2; Extended Data Figure 5).

The overall IBD analysis of 238 BoDV-1 sequences with available location suggested a significant positive correlation between geographic and genetic distance (Mantel test $p<0.0001$). This positive correlation was also found for the individual BoDV-1 clusters ($p\leq0.0028$; Extended Data Figure 8A).

Detailed spatial analysis of BoDV-1 phylogenetic clusters and subclusters

For a detailed analysis of the spatial distribution of BoDV-1, subtrees of individual clusters or subclusters were extracted from the BoDV-1 N-X/P ML tree (Figure 3A; Extended Data Figure 5) and all cases with available location were mapped geographically (Figure 3B to 3G). To aid visualization of relationships between phylogenetic analysis and geographic mapping, we indicated monophyletic subclades showing associations to particular geographic regions (Figure 3; Extended Data Figure 5).

The spatial distribution of subcluster 1A covers parts of southeastern BY as well as an area from southwestern BY to eastern Baden-Wuerttemberg (BW; Figure 3B; Extended Data Figure 5A). This bipartite distribution is also reflected by the phylogenetic pattern. The sequences from southeastern BY are located on a common branch that is subdivided into three phylogenetically and spatially distinguishable subclades (1A.SE-1, -2 and -3) covering distinct regions in southeastern BY with only minor overlaps among each other. The sequences from southwestern BY form a separate subclade (1A.SW). A further subclade is constituted by four sequences from BW (1A.BW-1), while the phylogenetic position of the fifth sequence from BW (1A.BW-2) is separated from all other sequences (Figure 3A; Extended Data Figure 5A).

Subcluster 1B is restricted to a rather confined region in the Alpine Rhine valley in the Swiss cantons Grisons (GR) and St. Gall (SG), with a few cases detected across the border into Liechtenstein (Figure 3C). The subcluster can be subdivided into a southern and a northern subclade (1B.S and 1B.N, respectively; Figure 3C; Extended Data Figure 5B). In this study, we were able to generate only one new sequence of subcluster 1B, which originated from the canton Thurgau (TG), a neighbouring canton of SG that has not been described as endemic for BoDV-1 so far. In agreement with its separate

location, the phylogenetic position of this sequence is basal to subclades 1B.S and 1B.N (Figure 3C; Extended Data Figure 5B).

Cluster 2 occupies major parts of central BY, mainly covering the region between the two parts of the dispersal area of subcluster 1A (Figures 1B and 3D; Extended Data Figure 5C). The cluster can be subdivided into three monophyletic subclades in the southwestern part of this area (2.SW-1, -2 and -3) and one that is mainly found more to the northeast in central Bavaria (2.MID) with only a few overlapping cases (Figure 3D; Extended Data Figure 5C).

Cluster 3 is situated mainly in eastern ST and in the South of SN, with single outliers in other federal states (Figure 3E; Extended Data Figure 5D). We assigned two phylogenetically supported subclades with, however, strongly overlapping dispersal areas (3.GG and 3.RO, named after the locations of the majority of their mainly shrew-derived sequences, Güterglück and Rosslau, respectively). The remaining sequences could not be assigned to prominent phylogenetic subclades (Figure 3E, Extended Data Figure 5D).

Cluster 4 is the most widely distributed cluster with a scattered geographic range covering parts of Upper Austria (UA), northern and southeastern BY, ST and BB. Individual additional cases were located in Schleswig-Holstein (SH), NI, Thuringia (TH), Hesse (HE) and BW (Figure 3F; Extended Data Figure 5E). In agreement with this geographic pattern, sequences of cluster 4 form several subclades with apparent association with distinct regions in UA (4.UA), southeastern and northern BY (4.BY-SE, 4.BY-N-1 and -2) and BB (4.BB). No clear subclades could be defined for a large group of genetically rather diverse sequences from northern parts of Germany (Figure 3E; Extended Data Figure 5E).

Both sequences of the newly identified cluster 5 originated from two neighbouring districts in a region in southern BY where usually sequences of cluster 2, subclades 2.SW-1 and -2 were found (Figures 1B, 3D and 3G; Extended Data Figure 5F).

Definition and further analysis of phylogeographic outliers

While phylogenetic grouping and geographic mapping were in good agreement with each other for the majority of BoDV-1 sequences, singular sequences appeared to be located distant from their

phylogenetic relatives (Figure 3). We sought for objectifiable and reproducible criteria to define such sequences as phylogeographic outliers. Pairwise nt comparisons of all N-X/P sequences with available location (n=238) showed that all sequences possessed one or more relatives with at least 98.6% nt sequence identity, with only one exception (Extended Data Figure 9A). The minimum distances of each case to all sequences with at least 98.6% nt sequence identity ranged from 0 to 366 km, with the 90th percentile at 37.9 km (Extended Data Figure 9B). Based on these observations, all cases without a sequence of at least 98.6% nt identity within a maximum distance of 37.9 km were marked as outliers, corresponding to the approximately 10% sequences with the highest minimal spatial distance to any close relative. These criteria were met by 24 of the 238 N-X/P sequences (10.1%; Figure 3; Extended Data Figure 5; Extended Data Table 3). Removal of outlier sequences from the IBD analysis increased the correlation coefficient (r), which measures the strength and direction of the correlation between genetic and geographic distance, for all clusters with the exception of cluster 1B. This effect was most prominent for cluster 2 (Extended Data Figure 8B).

For four of these outliers (outliers A, B, K and L), the available records revealed potential epidemiological links to areas where the respective BoDV-1 variants were considered to be endemic (Extended Data Table 3). A horse (outlier A; accession OR468845) had developed Borna disease in 2019 in North Rhine-Westphalia (NW), which is not known to be endemic for BoDV-1. The animal had been purchased from an endemic region in southwestern BY approximately two months before its death. In line with this information, the BoDV-1 N-X/P sequence from this horse belonged to subclade 1A.SW and it was identical to a sequence from a sheep from south-western BY in 2009 (OR468934; Figure 3B; Extended Data Figure 5A; Extended Data Table 3). An alpaca stallion from northern BY in 2022 (outlier B; OR468886) had been bought eight months before death from a region in southeastern BY, which is consistent with its BoDV-1 sequence belonging to subclade 1A.SE-2 (Figure 3B; Extended Data Figure 5A; Extended Data Table 3). The animal showed ataxia already on arrival at the new herd, which was assumed to be of orthopaedic cause. An additional alpaca stallion (outlier K; GQ861449) had developed disease in 2008 after having been transported from southwestern BY to the north of HE [21]. The BoDV-1 sequence from this case belonged to subclade 2.SW-1, which is in congruence with an infection

source in south-western BY (Figure 3C; Extended Data Figure 5B; Extended Data Table 3). Outlier L (OR468852), a horse from northern BY in 2021, had been bought from a horse trader in BW two weeks before death. The horse was reported to have been bought by the trader several weeks before from a not further specified location in BY. The BoDV-1 sequence of subclade 2.SW-1 suggests an infection source in south-western BY (Figure 3C; Extended Data Figure 5B; Extended Data Table 3).

In contrast, no epidemiological link to a potentially aberrant location of infection could be identified for the majority of the 24 identified outliers. In some cases, the available information suggested that the animal had never been in a region considered endemic for the respective BoDV-1 variant (outliers J, P, U), but in most cases the available information was insufficient. In some cases, the accuracy of the location data was low, e.g. representing the owner´s address, which may be distant from the actual husbandry (Extended Data Table 3). The human case Z19_0093 from western BY in 2016 (outlier F; OR468948) was classified as an outlier, since its sequence possessed only up to 98.1% nt identity to any other BoDV-1 sequence.

Two further RT-qPCR-confirmed BoDV-1 infections in horses were detected far from any known BoDV-1-endemic region. These cases had occurred in western Switzerland (canton Geneva [GE]) in 1988 and in eastern BB in 2006 (Figure 1B). However, sequencing attempts had failed due to poor RNA quality. Epidemiological data were not available for these cases.

Phylogeographic relationship of human- and animal-derived BoDV-1 sequences.

Of the 43 non-transplant-derived human BoDV-1 infections confirmed to date, 40 were diagnosed in BY, two in BB and one in TH (Figures 1B and 3). The vast majority of their BoDV-1 sequences matched the phylogenetic subclades found in the respective patient´s region of residence (Figure 3). Typically, sequences originating from animals or humans in close geographic proximity were representing the genetically closest relatives of human-derived sequences. For 90% of human-derived N-X/P sequences with available location (n=39), the distance to their phylogenetically closest relatives was less than 40 km, with a median distance of 15.6 km (Figure 4). In several cases, almost completely identical animal-derived sequences were found within less than 10 km distance to the residency of the human patient.

For instance, the human BoDV-1 sequence Z21_0129 (OR468964; subclade 1A.SW) shared 99.9% nt sequence identity with the horse-derived sequence OR468847 (NRL.20_085) that originated from the same district in south-eastern BY (Extended Data Figure 5A). Similarly, human sequence Z19_0107 (MT515369; cluster 3) [12] was 99.9% identical to that of an alpaca (NRL.22_102; OR468885) from the same district in BB (Extended Data Figure 5C). The BoDV-1 N-X/P sequences from patients Z19_0100 (MT364324) [11, 15] and Z20_0121 (OR468959) were completely identical among each other (99.9% at complete genome level) and 99.9% identical to the sequence of sheep NRL.21_092.12 (OR468866) from the same district in southeastern BY (Extended Data Figure 5A).

Besides outlier F mentioned above, only one additional human sequence was classified as an outlier. The BoDV-1 sequence of patient Z19_0086 (OR468945; outlier N; Extended Data Table 3) from southwestern BY belonged to cluster 3 and was, thus, genetically clearly different from all other sequences originating from this area. Its sequence was almost identical (99.9%) to the sequence of the vaccine strain 'DessauVac' (Extended Data Figure 5C). The precise origin of this historic vaccine strain is unknown, but it is believed to have been isolated from a horse from ST or western SN around 1949 [29, 37]. The closest relative of sequence Z19_0086 with available location originated from an alpaca in SN (MT366065) from about 370 km from the patient´s residency (Extended Data Table 3; Figure 4). Information on possible epidemiological links to ST or SN was not available. Likewise, no information was available on potential contacts of patient Z19_0086 to the vaccine strain DessauVac, which had been used until 1992 in eastern parts of Germany (former German Democratic Republic), but never in Bavaria. The sequence of case Z21_0139 from TH, 2021 (OK142783; marked as potential outlier Y) [13], showed likewise a high spatial distance to its most closely related BoDV-1 sequences. Its sequence belonged to subclade 4.BB and possessed up to 99.9% nt sequence identity to animal sequences from BB that are located more than 200 km from the patient´s home (Figure 4). However, since less closely related additional cluster 4 sequences (99.3% nt sequence identity) were found at a distance of roughly 25 km, the case did not match our criteria for a phylogeographic outlier.

Interestingly, both patients infected with BoDV-1 of cluster 5 had died after developing disease in 2002 and both lived in neighbouring districts in the vicinity of Munich (BY; Figure 3G; Extended Data Figure 5F). Cluster 5 has not been detected in shrews or domestic mammals so far.

Determination of BoDV-1 endemic areas

To visualize the endemic areas of each BoDV-1 cluster or subcluster, we employed KDE (Figure 1C). For this approach, all phylogeographic outliers defined above (Extended Data Table 3) were excluded from the dataset. The resulting KDE illustrated that the distribution of each BoDV-1 cluster or subcluster covered largely separated areas with little overlap (Figure 1C). In a second approach, we repeated the KDE using the combined dataset of all BoDV-1 clusters. This combined KDE revealed a tripartite endemic area (Figure 1D). The northernmost part ranges from northwestern BB to southern ST, possibly also including northern TH. The largest part covers most of BY and extends into BW and UA. The southernmost endemic area is found in the Alpine Rhine valley (Figure 1D). In addition, individual sequences not classified as outliers are found in NI south of Hamburg and in the Ore Mountains in SN, close to the Czech border (Figure 1D).

Discussion

The aim of this study was to assemble the most comprehensive data on the molecular epidemiology and phylogeography of BoDV-1 to allow for the identification of risk areas for the occurrence of spill-over transmission to domestic mammals and humans. Detection of BoDV-1 in shrews as the only known reservoir hosts would provide the most accurate information on its endemic presence. However, representative samples from the shrew host are not easily accessible. To date, these data are highly fragmented and biased due to active sampling at only a few locations [4, 24, 30, 31, 32, 33, 41]. We therefore adopted a passive surveillance approach, utilizing Borna disease in domestic mammals as an indicator of endemic BoDV-1 infection in local shrew populations. This approach may provide a potentially less biased fundament for phylogeographic analyses, although some variability of the dissemination of susceptible domestic animal populations and of veterinary vigilance within and outside of known endemic areas cannot be excluded. Reliable information on the location of infected individuals, not only during onset of disease but even more importantly, at the potential time point of infection, is crucial for this study. However, due to the long and possibly highly variable incubation period, such information is not always available, particularly for cases from earlier decades. Despite our extensive efforts to fill these data gaps, there are still varying degrees of uncertainty that must be considered when interpreting the results of this study.

Our analyses stably supported the previously introduced phylogenetic clusters and subclusters [37, 38, 39], for which we established objectifiable demarcation criteria, based on pairwise nt sequence identities of complete coding BoDV-1 genomes. The identification of a novel BoDV-1 cluster 5, represented by two human sequences from BY, indicates that the genetic variability of BoDV-1 may be higher than currently appreciated and that additional variants may exist within or outside the known endemic areas.

As demonstrated previously, we found the BoDV-1 clusters and subclusters to be genetically remarkably stable over time and to be associated with spatial distribution rather than time of detection or host species [7, 24, 37, 39]. In our study, we were able to markedly increase the extent, reliability and

resolution of the phylogeographic data, showing that BoDV-1 sequences of particular subclades are occupying circumscribed areas within the endemic regions. This geographically bound epidemiology further emphasizes that BoDV-1 is tied to a reservoir with a strictly territorial behaviour and only very little mobility [37,39]. Bicolored white-toothed shrews are known to occupy territories of 40 to 120 metres in diameter. They typically do not move more than 800 m to 1 km from their territory, with a documented maximum of 2.5 km, thus allowing for only limited virus spread [35]. This spatial limitation also underlines the fact that spill-over hosts, such as domestic mammals and humans, which tend to be more mobile, serve as dead-end hosts for the virus. Otherwise, their contribution to virus spread would have resulted in a much wider distribution of confirmed cases with considerable spatial overlap of genetic variants. Thus, our results very clearly support previous work [34,38,39,68] and refute former hypotheses of a possible worldwide spread of BoDV-1 among humans and non-reservoir animals [69,70].

To indicate the regions in which BoDV-1 variants of particular clusters or subclusters are endemic, we defined criteria for those sequences that indicate the endemic presence of the virus with reasonable reliability. Due to the limitations described above, a single BoDV-1 detection in a domestic mammal or human spatially separated from its closest viral relative cannot be considered as an indicator of endemicity. It rather needs to be supported by additional genetically related sequences from the same region. We have tentatively defined the criteria for considering sequences as indicators of endemicity to be at least two sequences with at least 98.6% nt sequence identity within a 37.9 km diameter. Applying these criteria, the approximately 10% of the sequences with the highest spatial distance from their closest relatives are regarded as phylogeographic outliers and excluded from further analysis. However, these criteria may be subject to further refinement as more extensive data will become available in future studies. Visualization of the distribution of the included sequences confirmed and refined the previously assumed pattern of endemic areas [34], but also extended it in certain regions, such as northern BY and eastern BW.

Geographic outliers do occasionally occur distant from the indicated distribution areas of their phylogenetic clades or even completely outside the defined endemic area of BoDV-1. Due to the

559 limitations of the available metadata, it cannot be excluded that at least some of these cases may be
560 the result of inaccurate locations. Others may be the result of travel within the incubation period, as
561 described previously [21, 22]. During the course of this study, at least three additional cases were
562 identified in which animals were likely to have been moved to new locations during the incubation
563 period, with BoDV-1 sequences suggesting sources of infection at the respective sites of origin. In one
564 of these cases, the alpaca had been moved no less than eight months prior to death. However, the
565 incubation period may have been shorter, as the animal was exhibiting a potentially BoDV-1-associated
566 ataxia already at the time of transfer.

567 Such clear epidemiological links could not be established for the majority of phylogeographic outliers
568 identified in this study. While no further information was available for most of these cases, some
569 animals were reported to have never travelled to known endemic areas, or even to have remained in
570 their holding of birth throughout their lives, thus suggesting the existence of so far unidentified
571 infection sources in these regions. Whether or not BoDV-1 can be transmitted over long distances by
572 passive vectors, such as import of contaminated feed, remains elusive. So far, no such cases have been
573 documented and data on the tenacity of the virus is sparse. Thus, at least some of the latter cases may
574 actually indicate the endemic presence of the virus in local shrew populations, requiring confirmation
575 by detection of additional genetically related viruses from their region. For instance, the phylogenetic
576 analyses of the previously published human case Z19_0107 from BB had grouped the virus to cluster
577 3 that had not been detected in this region before [12], suggesting a possibly aberrant infection source.
578 The recent detection of a highly similar BoDV-1 sequence from an alpaca from the same district in BB
579 now rather suggests endemicity of this BoDV-1 variant in this region and a peridomestic infection of
580 both individuals, which is also in accordance with the patient´s epidemiological history during the last
581 years before onset of the disease [12].

582 Our study increases the number of published laboratory-confirmed human BoDV-1-infections to 46
583 and provides a first comprehensive summary of metadata for all published cases [6, 7, 8, 9, 10, 11, 12, 13, 14, 15,
584 16, 17, 18]. The cases covered all age groups and encephalitis was diagnosed for 45 of the 46 patients, of

585 whom 44 had died as a result of the disease, resulting in a known case-fatality rate of 97.8%. As of
586 now, the accuracy of these numbers is difficult to assess. Many cases in this study were diagnosed only
587 by retrospective analysis of encephalitis cases and it is likely that particularly in the past a considerable
588 proportion of fatal BoDV-1 infections remained undetected [7]. This proportion may have been
589 comparably higher for possible non-fatal infections due to a lower alertness of physicians to such cases
590 and to the limited availability of diagnostic material for direct *intra vitam* detection of BoDV-1 , which
591 is hampered by the remarkable restriction of BoDV-1 to the central nervous system in erroneous spill-
592 over hosts [1, 7, 9, 20, 24, 34, 71]. However, the estimated prevalence of bornavirus-reactive antibodies did not
593 exceed 0.24% in recent serological surveys of healthy individuals or neuropsychiatric patients in known
594 endemic areas [65, 67, 72]. Analysis of brain tissue from encephalitis cases of unknown origin failed to
595 detect BoDV-1 in biopsy samples from 15 non-fatal cases, while BoDV-1 was detected in seven out of
596 nine (78%) fatal cases from the same cohort [7]. Likewise, nation-wide screenings identified bornavirus-
597 reactive antibodies in serological samples and/or BoDV-1 RNA in CSF only in patients suffering from
598 severe or fatal encephalitis [11, 65]. These findings support the assumption that non-fatal or even
599 asymptomatic human BoDV-1 infections are indeed at least very rare.

600 The detailed phylogeographic network of animal-derived BoDV-1 sequences assembled in this study
601 also allowed for a first phylogenetic assessment of potential geographic sources of human BoDV-1
602 infections. With the exception of three organ transplant-derived infections [88], all known infections are
603 assumed to have resulted from individual zoonotic spill-over events from the virus reservoir [6, 7, 9, 10, 11,
604 12], even though concrete transmission events could not be identified in a retrospective epidemiological
605 analysis of 20 cases [17]. Almost all human BoDV-1 sequences clustered in accordance with the location
606 of the patient´s residence. The median estimated distance to the closest phylogenetic relatives was
607 15.6 km, indicating that infection of most patients occurred close to home, which is in accordance with
608 epidemiological work identifying rural residence on the fringe of the settlement as the major risk factor
609 for BoDV-1 infection [17]. The actual distance to the source of infection is likely to be even lower in many

610 cases, since inaccuracies of location data, as well as unavailability of further sequences representing
611 genetically closer relatives are likely to lead to overestimation rather than underestimation.

612 The exact source and route of transmission remain elusive for almost all BoDV-1 infections in humans
613 and domestic mammals. Due to its almost exclusively neurotropic nature in non-reservoir hosts [7, 9, 20,
614 24, 71], transmission chains between spill-over hosts can be virtually excluded, with the exception of a so
615 far singular iatrogenic transmission event by solid organ transplantation [8]. This leaves infected shrews
616 as the most likely infection source. So far, it remains unknown whether exposure to their excretions is
617 sufficient for transmission or whether direct contact to an infected shrew or its carcass is required. In
618 a previous study, household members of deceased patients could not recollect potential events of
619 BoDV-1 exposure, indicating that these may be rather unremarkable [17]. Experimentally, BoDV-1
620 infection in animal models may be established via mucosal surfaces, mainly intranasally, or by
621 subcutaneous injection, followed by axonal spread to the brain via nerves and olfactory bulb or spinal
622 cord [73, 74, 75, 76, 77]. Overall, spill-over transmission of BoDV-1 to humans appears to be rather inefficient,
623 as only isolated cases have been reported so far. Associated infections of potentially equally exposed
624 individuals, such as family members or co-workers on agricultural farms, have not been detected, yet.
625 While the disease usually affects only a single animal or a small number of individuals in herds of horses
626 and sheep, higher incidences of BoDV-1 infections have been observed during outbreaks in New World
627 camelid holdings, leading to mortality rates of up to 40% within a few months in affected herds [24, 37, 39,
628 42]. Similarly, four out of eight alpacas of a herd from central BY analysed in our study succumbed to
629 confirmed BoDV-1 infection within one year (cases 21_013, 21_149.a, 22_015.a and 22_015.b;
630 Extended Data Figure 5C).

631 Previous studies have hypothesized a higher risk of BoDV-1 transmission to domestic mammals during
632 winter, leading to disease outbreaks and eventually death during spring and early summer. Shrews
633 entering animal stables in search of feed have been suggested to be responsible for this pattern [32, 39].
634 In congruence with these assumptions, our assembled data suggested a peak of laboratory-confirmed
635 fatal Borna disease in domestic mammals during May and June. In contrast, no such seasonality was

observed for the time of death or first known hospitalization of the comparably limited number of human BoDV-1 cases, similar to findings in a previous study of 20 human cases [17]. However, any conclusions regarding the time of infection are complicated by the unknown incubation period and the variable disease progression. Furthermore, the time from infection to death of human patients is affected by attempted treatments and life-sustaining measures, which further increase the variability. A larger dataset of human BoDV-1 infections may be required to demonstrate whether their temporal distribution actually differs from the occurrence of BoDV-1 infection in domestic mammals.

In summary, we performed a highly comprehensive phylogeographic analysis of the occurrence of the zoonotic pathogen BoDV-1 in Central Europe. The improved resolution of the phylogeographic data will provide a basis for assessing potential locations and sources of BoDV-1 infection in animals and humans. The visualization of potential risk areas will allow for the implementation of prophylactic measures – mainly reducing the risk of exposure to the reservoir – in the affected regions. In such areas, BoDV-1 may be responsible for a considerable proportion of cases of severe human encephalitis that may have remained unresolved so far [7]. Increased awareness among veterinarians and physicians, together with the categorization of BoDV-1 as a notifiable pathogen of humans and animals since 2020 [11], may lead to more extensive data collection, allowing for further refinement of phylogeographic analyses in the future.

Acknowledgments

We would like to thank Patrick Zitzow, Kathrin Steffen, Weda Hoffmann, Lukas Wessler, Jessica Geers and Elsbeth Keller-Gautschi for their outstanding technical assistance. Brigitte Böhm, Eva Kappe (both Poing, Germany), Wolfram Breuer, Melanie Bühler, Anne Kupca (all Oberschleissheim, Germany), Gesine Buhmann, Karin Weber (both Munich, Germany), Klaus-Jürgen Danner (Freiburg, Germany), Vanessa Franzen (Munich, Germany), Sascha Gerst (Rostock, Germany), Ernst Großmann (Aulendorf, Germany), Wolfram Haider (Berlin, Germany), Anja Heinrich, Claudia Kiesow (both Stendal, Germany), Christian Imholt, Jens Jacob, Philipp Koch (Münster, Germany), Andrea Konrath, Martin Pfeffer (Leipzig, Germany), Martin Peters (Arnsberg, Germany), Dietrich Pöhle (Dresden, Germany), Ingo Schwabe (Fellbach, Germany), Christoph Schulze (Frankfurt/Oder, Germany), Herbert Weissenböck (Vienna, Austria) and Eva-Maria Wittauer (Bad Kissingen, Germany) submitted diagnostic material from confirmed or suspected cases of Borna disease or BoDV-1-infected shrews. Furthermore, we like to thank all veterinarians and physicians treating the analysed animals and human patients, respectively. We are grateful to Sybille Herzog (Giessen, Germany) for providing BoDV-1 isolates for re-sequencing, Sven Springer (IDT Biologika, now Ceva Santé Animale, Dessau-Rosslau, Germany) for kindly providing a vial of the bornavirus live vaccine ‘Dessau’ and Christiane Herden (Giessen, Germany) for providing the laboratory strain H24. We like to thank Dirk Höper for providing funding, technical supervision and advice as well as for critically discussing the data analysis and the manuscript.

Funding

This work was supported by the Federal Ministry of Education and Research within the research consortium “ZooBoCo” (Grant no. 01KI1722 and 01KI2005 donated to Martin Beer, Dirk Höper, Timo Homeier-Bachmann, Kirsten Pörtner, Dennis Rubbenstroth, Dennis Tappe and Rainer G. Ulrich) and the projects “ZooKoInfekt” (01KI1903B; Rainer G. Ulrich and Dennis Rubbenstroth) and "Bornavirus - Focal Point Bavaria" (01KI2002; Barbara Schmidt). Friederike Liesche-Starnecker received funding from the German Research Foundation (DFG; no. 504757758).

Statement of Data Availability

All novel BoDV-1 sequences are available from the INSDC databases under accession numbers OR203629, OR203630, OR468838 to OR468971. Reanalysed previously published isolates (H640 and H3053) are available under accession numbers AY374523.2 and AY374537.2.

Ethics Statement

Ethical approval of the analysis of archived human samples was obtained from the local ethical commission of the Faculty for Medicine, University of Regensburg (ref. no. 18-1248-101), the Technical University Munich (577/19 S), the Ludwigs-Maximilians University Munich (23-0267) and the Medical Board of Hamburg (PV5616). Samples of BoDV-1-positive bicolored white-toothed shrews were obtained from an ongoing large-scale small mammal screening study (Haring et al., manuscript in preparation). Shrew KS20/0026 originated from a project that was commissioned by the Federal Environment Agency as part of the Environmental Research Plan (Research Code 3718 48 4250; animal ethics permit: 42502-2-1548 UniLeipzig) and was financed with federal funds. All other shrew carcasses included in this study were found dead or preyed by cats. Samples from domestic mammals originated from diagnostic necropsies. No living animals were handled or killed for the purpose of this study.

Conflict of interest

The authors declare no conflicts of interest. The funders played no role in the design of the study, in the collection, analysis, or interpretation of the data, in the writing of the manuscript, or in the decision to publish the results.

References

1. Dürrwald R, Nowotny N, Beer M, Kuhn JH. Infections caused by Bornaviruses. In: *Clinical Virology* (eds Richman DD, Whitley RJ, Hayden FG). 4th edition edn. American Society for Microbiology (2016).

2. Richt JA, Rott R. Borna disease virus: a mystery as an emerging zoonotic pathogen. *Vet J* **161**, 24-40 (2001).

3. Staeheli P, Sauder C, Hausmann J, Ehrensperger F, Schwemmle M. Epidemiology of Borna disease virus. *J Gen Virol* **81**, 2123-2135 (2000).

4. Weissenböck H, Bago Z, Kolodziejek J, Hager B, Palmetzhofer G, Dürrwald R, Nowotny N. Infections of horses and shrews with bornaviruses in Upper Austria: a novel endemic area of Borna disease. *Emerg Microbes Infect* **6**, e52 (2017).

5. Rubbenstroth D*, et al.* ICTV Virus Taxonomy Profile: *Bornaviridae*. *J Gen Virol* **102**, 001613 (2021).

6. Korn K*, et al.* Fatal Encephalitis Associated with Borna Disease Virus 1. *N Engl J Med* **379**, 1375-1377 (2018).

7. Niller HH*, et al.* Zoonotic spillover infections with Borna disease virus 1 leading to fatal human encephalitis, 1999-2019: an epidemiological investigation. *Lancet Infect Dis* **20**, 467-477 (2020).

8. Schlottau K*, et al.* Fatal encephalitic Borna disease virus 1 in solid-organ transplant recipients. *N Engl J Med* **379**, 1377-1379 (2018).

9. Liesche F*, et al.* The neuropathology of fatal encephalomyelitis in human Borna virus infection. *Acta Neuropathol* **138**, 653-665 (2019).

10. Coras R, Korn K, Kuerten S, Huttner HB, Ensser A. Severe bornavirus-encephalitis presenting as Guillain-Barre-syndrome. *Acta Neuropathol* **137**, 1017-1019 (2019).

11. Eisermann P*, et al.* Active Case Finding of Current Bornavirus Infections in Human Encephalitis Cases of Unknown Etiology, Germany, 2018-2020. *Emerg Infect Dis* **27**, 1371-1379 (2021).

12. Tappe D*, et al.* Investigation of fatal human Borna disease virus 1 encephalitis outside the previously known area for human cases, Brandenburg, Germany - a case report. *BMC Infect Dis* **21**, 787 (2021).

13. Frank C*, et al.* Human Borna disease virus 1 (BoDV-1) encephalitis cases in the north and east of Germany. *Emerg Microbes Infect* **11**, 6-13 (2022).

14. Meier H*, et al.* [Bornavirus encephalitis as a differential diagnosis to seronegative autoimmune encephalitis]. *Nervenarzt* **93**, 835-837 (2022).

15. Grosse L*, et al.* First detected geographical cluster of BoDV-1 encephalitis from same small village in two children: therapeutic considerations and epidemiological implications. *Infection*, 10.1007/s15010-023-01998-w, 1-16 (2023).

16. Neumann B*, et al.* Antibodies against viral nucleo-, phospho-, and X protein contribute to serological diagnosis of fatal Borna disease virus 1 infections. *Cell Rep Med* **3**, 100499 (2022).

17. Pörtner K, Wilking H, Frank C, Bohmer MM, Stark K, Tappe D. Risk factors for Borna disease virus 1 encephalitis in Germany - a case-control study. *Emerg Microbes Infect* **12**, e2174778 (2023).

18. Liesche-Starnecker F*, et al.* Hemorrhagic lesion with detection of infected endothelial cells in human bornavirus encephalitis. *Acta Neuropathol* **144**, 377-379 (2022).

19. Stitz L, Bilzer T, Planz O. The immunopathogenesis of Borna disease virus infection. *Front Biosci* **7**, d541-555 (2002).

20. Fürstenau J*, et al.* Borna disease virus 1 infection in alpacas: Comparison of pathological lesions and viral distribution to other dead-end hosts. *Vet Pathol*, 10.1177/03009858231185107, 3009858231185107 (2023).

21. Jacobsen B*, et al.* Borna disease in an adult alpaca stallion (*Lama pacos*). *J Comp Pathol* **143**, 203-208 (2010).

22. Priestnall SL*, et al.* Borna disease virus infection of a horse in Great Britain. *Vet Rec* **168**, 380b (2011).

23. Caplazi P, Melzer K, Goetzmann R, Rohner-Cotti A, Bracher V, Zlinszky K, Ehrensperger F. [Borna disease in Switzerland and in the principality of Liechtenstein]. *Schweiz Arch Tierheilkd* **141**, 521-527 (1999).

24. Schulze V*, et al.* Borna disease outbreak with high mortality in an alpaca herd in a previously unreported endemic area in Germany. *Transbound Emerg Dis* **67**, 2093-2107 (2020).

25. Jordan I, Briese T, Averett DR, Lipkin WI. Inhibition of Borna disease virus replication by ribavirin. *J Virol* **73**, 7903-7906 (1999).

26. Lee BJ, Matsunaga H, Ikuta K, Tomonaga K. Ribavirin inhibits Borna disease virus proliferation and fatal neurological diseases in neonatally infected gerbils. *Antiviral Res* **80**, 380-384 (2008).

27. Reuter A*, et al.* Synergistic antiviral activity of ribavirin and interferon-alpha against parrot bornaviruses in avian cells. *J Gen Virol* **97**, 2096-2103 (2016).

28. Tokunaga T, Yamamoto Y, Sakai M, Tomonaga K, Honda T. Antiviral activity of favipiravir (T-705) against mammalian and avian bornaviruses. *Antiviral Res* **143**, 237-245 (2017).

29. Dürrwald R, Kolodziejek J, Oh DY, Herzog S, Liebermann H, Osterrieder N, Nowotny N. Vaccination against Borna Disease: Overview, Vaccine Virus Characterization and Investigation of Live and Inactivated Vaccines. *Viruses* **14**, 2706 (2022).

30. Hilbe M, Herrsche R, Kolodziejek J, Nowotny N, Zlinszky K, Ehrensperger F. Shrews as reservoir hosts of borna disease virus. *Emerg Infect Dis* **12**, 675-677 (2006).

31. Puorger ME, Hilbe M, Müller JP, Kolodziejek J, Nowotny N, Zlinszky K, Ehrensperger F. Distribution of Borna disease virus antigen and RNA in tissues of naturally infected bicolored white-toothed shrews, *Crocidura leucodon*, supporting their role as reservoir host species. *Vet Pathol* **47**, 236-244 (2010).

32. Dürrwald R, Kolodziejek J, Weissenböck H, Nowotny N. The bicolored white-toothed shrew *Crocidura leucodon* (HERMANN 1780) is an indigenous host of mammalian Borna disease virus. *PLoS One* **9**, e93659 (2014).

33. Nobach D, Bourg M, Herzog S, Lange-Herbst H, Encarnacao JA, Eickmann M, Herden C. Shedding of infectious Borna disease virus 1 in living bicolored white-toothed shrews. *PLoS One* **10**, e0137018 (2015).

34. Rubbenstroth D, Schlottau K, Schwemmle M, Rissland J, Beer M. Human bornavirus research: Back on track! *PLoS Pathog* **15**, e1007873 (2019).

35. Burgin CJ, He K. Family Soricidae (Shrews). In: *Handbook of the Mammals of the World: Insectivores, Sloths and Colugos* (eds Wilson DE, Mittermeier RA). Lynx Edicions (2018).

36. Krapp F. *Crocidura leucodon* (Herrmann, 1780) - Feldspitzmaus. In: *Handbuch der Säugetiere Europas [Handbook of European mammals]* (eds Niethammer J, Krapp F). Aula Verlag GmbH (1990).

37. Kolodziejek J, Dürrwald R, Herzog S, Ehrensperger F, Lussy H, Nowotny N. Genetic clustering of Borna disease virus natural animal isolates, laboratory and vaccine strains strongly reflects their regional geographical origin. *J Gen Virol* **86**, 385-398 (2005).

38. Dürrwald R, Kolodziejek J, Herzog S, Nowotny N. Meta-analysis of putative human bornavirus sequences fails to provide evidence implicating Borna disease virus in mental illness. *Rev Med Virol* **17**, 181-203 (2007).

39. Dürrwald R, Kolodziejek J, Muluneh A, Herzog S, Nowotny N. Epidemiological pattern of classical Borna disease and regional genetic clustering of Borna disease viruses point towards the existence of to-date unknown endemic reservoir host populations. *Microbes Infect* **8**, 917-929 (2006).

40. Rubbenstroth D, Schmidt V, Rinder M, Legler M, Twietmeyer S, Schwemmer P, Corman VM. Phylogenetic analysis supports horizontal transmission as a driving force of the spread of avian bornaviruses. *PLoS One* **11**, e0160936 (2016).

41. Bourg M, Herzog S, Encarnacao JA, Nobach D, Lange-Herbst H, Eickmann M, Herden C. Bicolored white-toothed shrews as reservoir for Borna disease virus, Bavaria, Germany. *Emerg Infect Dis* **19**, 2064-2066 (2013).

42. Malbon AJ*, et al.* New World camelids are sentinels for the presence of Borna disease virus. *Transbound Emerg Dis* **69**, 451-464 (2021).

43. Schlegel M, Ali HS, Stieger N, Groschup MH, Wolf R, Ulrich RG. Molecular identification of small mammal species using novel cytochrome B gene-derived degenerated primers. *Biochem Genet* **50**, 440-447 (2012).

44. Wylezich C, Papa A, Beer M, Höper D. A Versatile Sample Processing Workflow for Metagenomic Pathogen Detection. *Sci Rep* **8**, 13108 (2018).

45. Matiasek K*, et al.* Mystery of fatal 'staggering disease' unravelled: novel rustrela virus causes severe meningoencephalomyelitis in domestic cats. *Nat Commun* **14**, 624 (2023).

46. Toussaint JF, Sailleau C, Breard E, Zientara S, De Clercq K. Bluetongue virus detection by two real-time RT-qPCRs targeting two different genomic segments. *Journal of Virological Methods* **140**, 115-123 (2007).

47. Hoffmann B, Depner K, Schirrmeier H, Beer M. A universal heterologous internal control system for duplex real-time RT-PCR assays used in a detection system for pestiviruses. *Journal of Virological Methods* **136**, 200-209 (2006).

48. Ebinger A, Fischer S, Höper D. A theoretical and generalized approach for the assessment of the sample-specific limit of detection for clinical metagenomics. *Computational and Structural Biotechnology Journal* **19**, 732-742 (2020).

49. Szillat KP, Höper D, Beer M, König P. Full-genome sequencing of German rabbit haemorrhagic disease virus uncovers recombination between RHDV (GI.2) and EBHSV (GII.1). *Virus Evol* **6**, veaa080 (2020).

50. Shen W, Le S, Li Y, Hu F. SeqKit: A Cross-Platform and Ultrafast Toolkit for FASTA/Q File Manipulation. *PLoS One* **11**, e0163962 (2016).

51. Bankevich A*, et al.* SPAdes: a new genome assembly algorithm and its applications to single-cell sequencing. *J Comput Biol* **19**, 455-477 (2012).

52. Edgar RC. MUSCLE: multiple sequence alignment with high accuracy and high throughput. *Nucleic Acids Res* **32**, 1792-1797 (2004).

53. Minh BQ, Schmidt HA, Chernomor O, Schrempf D, Woodhams MD, von Haeseler A, Lanfear R. IQ-TREE 2: New models and efficient methods for phylogenetic inference in the genomic era. *Mol Biol Evol* **37**, 1530-1534 (2020).

54. Kalyaanamoorthy S, Minh BQ, Wong TKF, von Haeseler A, Jermiin LS. ModelFinder: fast model selection for accurate phylogenetic estimates. *Nat Methods* **14**, 587-589 (2017).

55. Hoang DT, Chernomor O, von Haeseler A, Minh BQ, Vinh LS. UFBoot2: Improving the Ultrafast Bootstrap Approximation. *Mol Biol Evol* **35**, 518-522 (2018).

56. Guindon S, Dufayard JF, Lefort V, Anisimova M, Hordijk W, Gascuel O. New algorithms and methods to estimate maximum-likelihood phylogenies: assessing the performance of PhyML 3.0. *Syst Biol* **59**, 307-321 (2010).

57. Yu G. Using ggtree to Visualize Data on Tree-Like Structures. *Current Protocols in Bioinformatics* **69**, e96 (2020).

58. RStudio Team. RStudio: Integrated Development for R (2020).

59. R Core Team. R: A Language and Environment for Statistical Computing (2020).

60. Kolde R. pheatmap: Pretty Heatmaps (2019).

61. Rambaut A, Lam TT, Max Carvalho L, Pybus OG. Exploring the temporal structure of heterochronous sequences using TempEst (formerly Path-O-Gen). *Virus evolution* **2**, vew007-vew007 (2016).

62. Massicotte P, South A. rnaturalearth: World Map Data from Natural Earth (2023).

63. Wickham H. *ggplot2: Elegant Graphics for Data Analysis*. Springer-Verlag New York (2016).

64. Venables WN, Ripley BD. *Modern Applied Statistics with S*, Fourth edn. Springer (2002).

65. Allartz P*, et al.* Detection of bornavirus-reactive antibodies and BoDV-1 RNA only in encephalitis patients from virus endemic areas: a comparative serological and molecular sensitivity, specificity, predictive value, and disease duration correlation study. *Infection*, 10.1007/s15010-023-02048-1, 1-13 (2023).

66. Neumann B*, et al.* Cerebrospinal fluid in Borna disease virus 1 (BoDV-1) encephalitis. *J Neurol Sci* **446**, 120568 (2023).

67. Bauswein M*, et al.* Human Infections with Borna Disease Virus 1 (BoDV-1) Primarily Lead to Severe Encephalitis: Further Evidence from the Seroepidemiological BoSOT Study in an Endemic Region in Southern Germany. *Viruses* **15**, (2023).

68. Rubbenstroth D, Niller HH, Angstwurm K, Schwemmle M, Beer M. Are human Borna disease virus 1 infections zoonotic and fatal? - Authors' reply. *Lancet Infect Dis* **20**, 651 (2020).

69. Ludwig H. Essentials in bornavirus virology - an epilogue. *APMIS Suppl* **124**, 94-97 (2008).

70. Bode L, Guo Y, Xie P. Molecular epidemiology of human Borna disease virus 1 infection revisited. *Emerg Microbes Infect* **11**, 1335-1338 (2022).

71. Bilzer T, Planz O, Lipkin WI, Stitz L. Presence of CD4+ and CD8+ T cells and expression of MHC class I and MHC class II antigen in horses with Borna disease virus-induced encephalitis. *Brain Pathol* **5**, 223-230 (1995).

72. Tappe D*, et al.* Low prevalence of Borna disease virus 1 (BoDV-1) IgG antibodies in humans from areas endemic for animal Borna disease of Southern Germany. *Sci Rep* **9**, 20154 (2019).

73. Kupke A, Becker S, Wewetzer K, Ahlemeyer B, Eickmann M, Herden C. Intranasal Borna disease virus (BoDV-1) infection: insights into initial steps and potential contagiosity. *Int J Mol Sci* **20**, 1318 (2019).

74. Carbone KM, Duchala CS, Griffin JW, Kincaid AL, Narayan O. Pathogenesis of Borna disease in rats: evidence that intra-axonal spread is the major route for virus dissemination and the determinant for disease incubation. *J Virol* **61**, 3431-3440 (1987).

75. Morales JA, Herzog S, Kompter C, Frese K, Rott R. Axonal transport of Borna disease virus along olfactory pathways in spontaneously and experimentally infected rats. *Med Microbiol Immunol* **177**, 51-68 (1988).

76. Sauder C, Staeheli P. Rat model of borna disease virus transmission: epidemiological implications. *J Virol* **77**, 12886-12890 (2003).

77. Krey H. Ocular involvement in BDV-infected rabbits and primates. *APMIS Suppl* **124**, 58-60 (2008).

Table 1. Numbers of cases and sequences included in this study.

Parameter	Domestic mammals [a]	Humans	Shrews	Laboratory strains [b]	Total
cases analysed in this study	231	29 [c]	7	2	269
fresh or fresh-frozen samples	48	14	7	2	71
FFPE samples	183	15	0	0	198
confirmed by RT-qPCR	207	28	7	n.a. [d]	242
comparative Mix-1/-6 results	204	23	7	n.a.	234
selected for sequencing	120	28	7	2	157
Sanger sequencing	31	5	7	0	43
high throughput sequencing	89	23	0	2	114
bait-based enrichment	14	2	0	0	16
cases with sequences	102	25	7	2	136
complete coding genomes [e]	36	16	0	2	54
at least N-X/P genes [e]	66	9	7	0	82
publicly available sequences					
total cases included	55	16	36	3	110
complete coding genomes [e]	9	15	10	2	36
at least N-X/P genes [e]	46	1	26	1	74
total cases included	286	47 [f]	43	5	381
confirmed BoDV-1 infections [g]	262	46 [f]	43	5	356
cases with sequences	157	41	43	5	246
coding-complete genomes	45	31	10	4	90
at least N-X/P genes	112	10	33	1	156
total cases with available location	278	43	42	2	365
confirmed with available location [g]	254	42	42	2	340
confirmed with available year [g]	262	46	n.a.	3	309
confirmed with available month [f]	257	45	n.a.	0	302
sequences with available location	155	39	42	2	238

[a] Domestic mammals also include two cases of non-domesticated zoo animals (pygmy hippopotamus).

[b] BoDV-1 isolates He/80, strain V, H24, H215 and DessauVac, which all originate from domestic mammals and have passaging histories in cell culture and/or experimental animals extending beyond the initial isolation in cell culture, were classified as laboratory strains. If more than one sequence per isolate was available, only the original sequence was included. The cell culture-derived materials from cases H640 and H3053 are not included in this table since they were used only for re-sequencing and correction of sequence database entries.

[c] Human samples analysed in this study originated from unpublished cases as well as from previously published cases without published BoDV-1 sequence [7, 9, 13, 14, 16, 17, 18, 65, 67].

[d] n.a. = not analysed

[e] Complete coding BoDV-1 genomes: 8,769 nucleotides, ranging from genome position 54 (start of the N gene) to 8,822 (end of the L gene); N-X/P sequences: 1,824 bp, ranging from position 54 to 1,877 (end of the P gene).

[f] In addition to the 29 human cases analysed during this study and the 16 human cases with publicly available sequences, two further published human cases without available sequence were regarded as confirmed human BoDV-1 infections based on their unequivocal epidemiological link in

983 combination with detectable seroconversion. These two patients are the donor and the surviving
984 liver recipient of the solid organ transplant cluster published by Schlottau et al. [8].

985 [g] Cases confirmed by either positive RT-qPCR result or publicly available sequences.

986

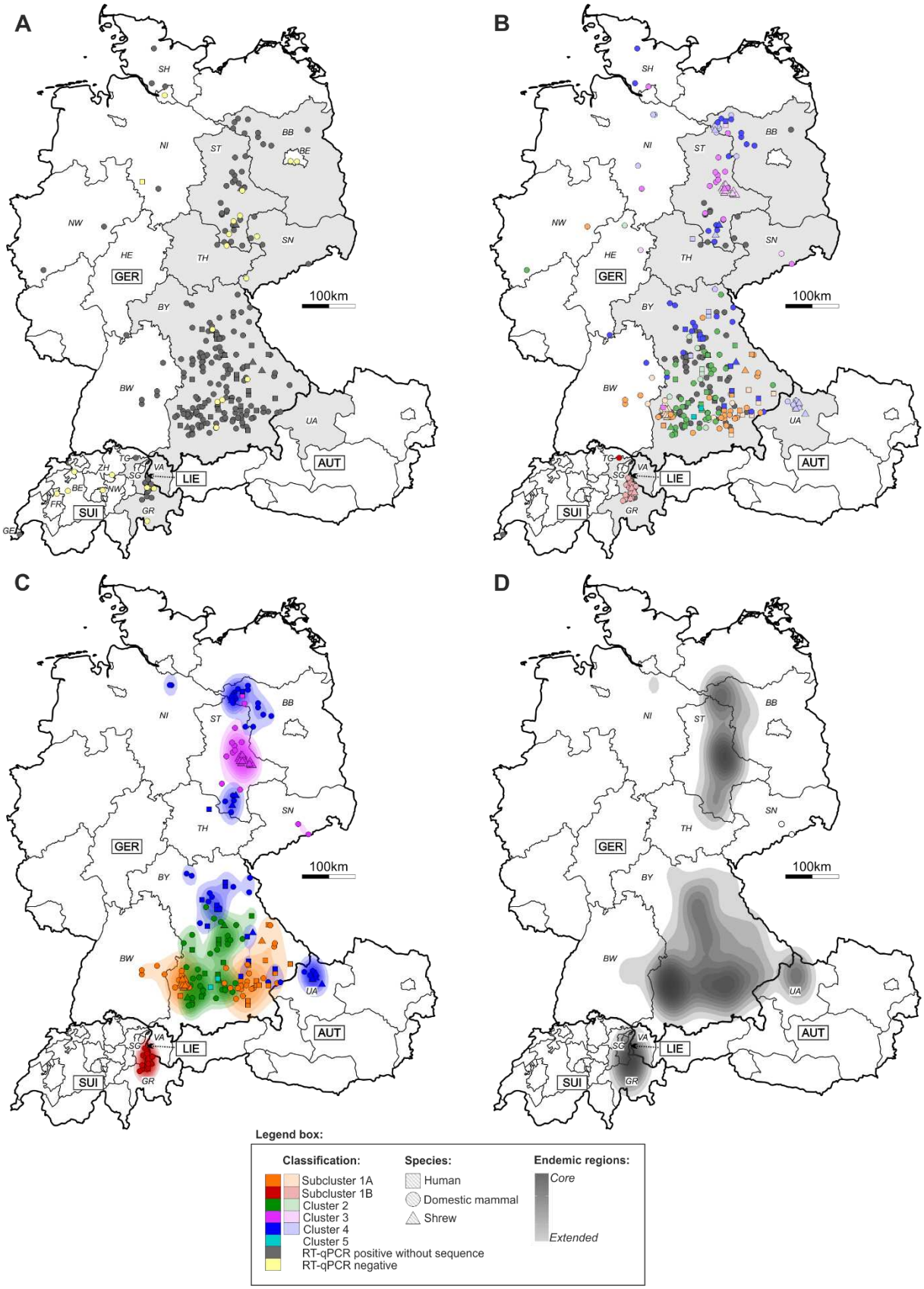
A
B
C
D
SH
NI
BB
ST
BE
NW
HE
TH
SN
GER
BY
BW
UA
AUT
LIE
SUI
GR
TG
VA
SG
FR
100km
Legend box:
Classification:
Subcluster 1A
Subcluster 1B
Cluster 2
Cluster 3
Cluster 4
Cluster 5
RT-qPCR positive without sequence
RT-qPCR negative
Species:
Human
Domestic mammal
Shrew
Endemic regions:
Core
Extended

987

988

Figure 1. Geographic location of analysed cases and BoDV-1 sequences. A) Origin of suspected or confirmed cases of Borna disease from domestic mammals and humans and of BoDV-1-infected shrews submitted for analysis. Grey symbols represent cases confirmed by BoDV-1-specific RT-qPCR in this study. Yellow symbols represent cases without a positive RT-qPCR result. The federal states (Germany, Austria) and cantons (Switzerland) coloured in light grey represent the assumed endemic regions based on previously published work [4, 7, 24, 32, 37, 42]. **B)** Geographic locations of BoDV-1 sequences originating from this study (dark colours) or previously published cases (light colours). Colours represent phylogenetic BoDV-1 clusters and subclusters as determined in Figures 2 and 3A and Extended Data Figure 5. Grey symbols represent cases confirmed by BoDV-1-specific RT-qPCR in this study without available sequence. **C)** Visualization of endemic regions of BoDV-1 clusters and subclusters by Kernel Density Estimation (KDE). The analysis is based on 214 BoDV-1 sequences with available location. Sequences classified as phylogenetic outliers (no additional sequence with at least 98.6% nucleotide sequence identity within a maximal distance of 37.9 km) were excluded from the analysis. **D)** Cluster-independent BoDV-1 endemic region visualized by KDE. Only sequences meeting the criteria described for panel C) were included. Germany (GER): BB = Brandenburg, BE = Berlin, BY = Bavaria, BW = Baden-Wuerttemberg, HE = Hesse, NI = Lower Saxony, NW = North Rhine-Westphalia, SH = Schleswig-Holstein, SN = Saxony, ST = Saxony-Anhalt, TH = Thuringia; Switzerland (SUI): BE = Bern, FR = Fribourg, GE = Geneva, GR = Grisons, NW = Nidwalden, SG = St. Gall, TG = Thurgau, ZH = Zurich; Austria (AUT): UA = Upper Austria, VA = Vorarlberg; Liechtenstein (LIE).

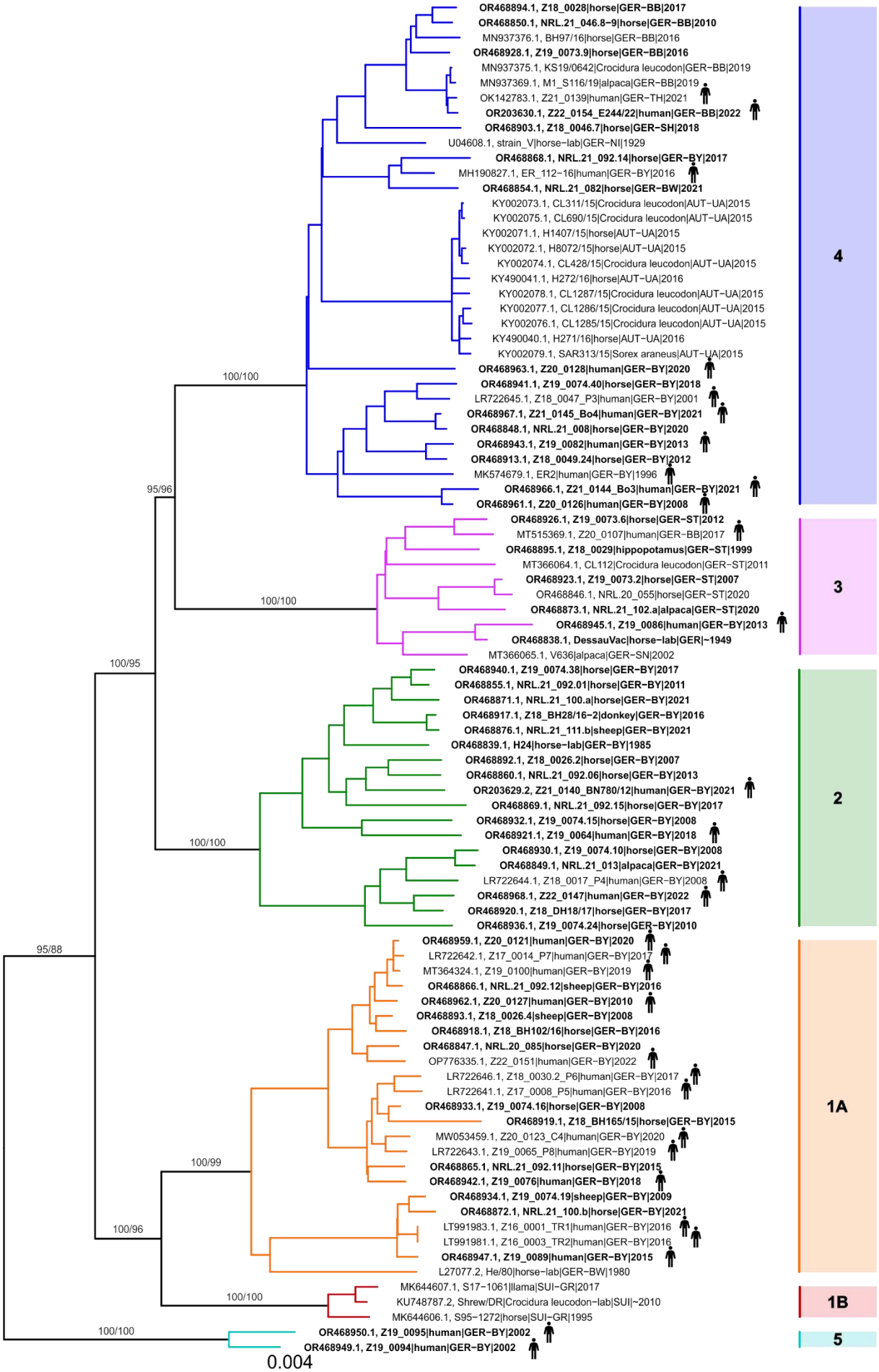
OR468894.1, Z18_0028|horse|GER−BB|2017
OR468850.1, NRL.21_046.8−9|horse|GER−BB|2010
MN937376.1, BH97/16|horse|GER−BB|2016
OR468928.1, Z19_0073.9|horse|GER−BB|2016
MN937375.1, KS19/0642|Crocidura leucodon|GER−BB|2019
MN937369.1, M1_S116/19|alpaca|GER−BB|2019
OK142783.1, Z21_0139|human|GER−TH|2021
OR203630.1, Z22_0154_E244/22|human|GER−BB|2022
OR468903.1, Z18_0046.7|horse|GER−SH|2018
U04608.1, strain_V|horse−lab|GER−NI|1929
OR468868.1, NRL.21_092.14|horse|GER−BY|2017
MH190827.1, ER_112−16|human|GER−BY|2016
OR468854.1, NRL.21_082|horse|GER−BW|2021
KY002073.1, CL311/15|Crocidura leucodon|AUT−UA|2015
KY002075.1, CL690/15|Crocidura leucodon|AUT−UA|2015
KY002071.1, H1407/15|horse|AUT−UA|2015
KY002072.1, H8072/15|horse|AUT−UA|2015
KY002074.1, CL428/15|Crocidura leucodon|AUT−UA|2015
KY490041.1, H272/16|horse|AUT−UA|2016
KY002078.1, CL1287/15|Crocidura leucodon|AUT−UA|2015
KY002077.1, CL1286/15|Crocidura leucodon|AUT−UA|2015
KY002076.1, CL1285/15|Crocidura leucodon|AUT−UA|2015
KY490040.1, H271/16|horse|AUT−UA|2016
KY002079.1, SAR313/15|Sorex araneus|AUT−UA|2015
OR468963.1, Z20_0128|human|GER−BY|2020
OR468941.1, Z19_0074.40|horse|GER−BY|2018
LR722645.1, Z18_0047_P3|human|GER−BY|2001
OR468967.1, Z21_0145_Bo4|human|GER−BY|2021
OR468848.1, NRL.21_008|horse|GER−BY|2020
OR468943.1, Z19_0082|human|GER−BY|2013
OR468913.1, Z18_0049.24|horse|GER−BY|2012
MK574679.1, ER2|human|GER−BY|1996
OR468966.1, Z21_0144_Bo3|human|GER−BY|2021
OR468961.1, Z20_0126|human|GER−BY|2008
OR468926.1, Z19_0073.6|horse|GER−ST|2012
MT515369.1, Z20_0107|human|GER−BB|2017
OR468895.1, Z18_0029|hippopotamus|GER−ST|1999
MT366064.1, CL112|Crocidura leucodon|GER−ST|2011
OR468923.1, Z19_0073.2|horse|GER−ST|2007
OR468846.1, NRL.20_055|horse|GER−ST|2020
OR468873.1, NRL.21_102.a|alpaca|GER−ST|2020
OR468945.1, Z19_0086|human|GER−BY|2013
OR468838.1, DessauVac|horse−lab|GER|~1949
MT366065.1, V636|alpaca|GER−SN|2002
OR468940.1, Z19_0074.38|horse|GER−BY|2017
OR468855.1, NRL.21_092.01|horse|GER−BY|2011
OR468871.1, NRL.21_100.a|horse|GER−BY|2021
OR468917.1, Z18_BH28/16−2|donkey|GER−BY|2016
OR468876.1, NRL.21_111.b|sheep|GER−BY|2021
OR468839.1, H24|horse−lab|GER−BY|1985
OR468892.1, Z18_0026.2|horse|GER−BY|2007
OR468860.1, NRL.21_092.06|horse|GER−BY|2013
OR203629.2, Z21_0140_BN780/12|human|GER−BY|2021
OR468869.1, NRL.21_092.15|horse|GER−BY|2017
OR468932.1, Z19_0074.15|horse|GER−BY|2008
OR468921.1, Z19_0064|human|GER−BY|2018
OR468930.1, Z19_0074.10|horse|GER−BY|2008
OR468849.1, NRL.21_013|alpaca|GER−BY|2021
LR722644.1, Z18_0017_P4|human|GER−BY|2008
OR468968.1, Z22_0147|human|GER−BY|2022
OR468920.1, Z18_DH18/17|horse|GER−BY|2017
OR468936.1, Z19_0074.24|horse|GER−BY|2010
OR468959.1, Z20_0121|human|GER−BY|2020
LR722642.1, Z17_0014_P7|human|GER−BY|2017
MT364324.1, Z19_0100|human|GER−BY|2019
OR468866.1, NRL.21_092.12|sheep|GER−BY|2016
OR468962.1, Z20_0127|human|GER−BY|2010
OR468893.1, Z18_0026.4|sheep|GER−BY|2008
OR468918.1, Z18_BH102/16|horse|GER−BY|2016
OR468847.1, NRL.20_085|horse|GER−BY|2020
OP776335.1, Z22_0151|human|GER−BY|2022
LR722646.1, Z18_0030.2_P6|human|GER−BY|2017
LR722641.1, Z17_0008_P5|human|GER−BY|2016
OR468933.1, Z19_0074.16|horse|GER−BY|2008
OR468919.1, Z18_BH165/15|horse|GER−BY|2015
MW053459.1, Z20_0123_C4|human|GER−BY|2020
LR722643.1, Z19_0065_P8|human|GER−BY|2019
OR468865.1, NRL.21_092.11|horse|GER−BY|2015
OR468942.1, Z19_0076|human|GER−BY|2018
OR468934.1, Z19_0074.19|sheep|GER−BY|2009
OR468872.1, NRL.21_100.b|horse|GER−BY|2021
LT991983.1, Z16_0001_TR1|human|GER−BY|2016
LT991981.1, Z16_0003_TR2|human|GER−BY|2016
OR468947.1, Z19_0089|human|GER−BY|2015
L27077.2, He/80|horse−lab|GER−BW|1980
MK644607.1, S17−1061|llama|SUI−GR|2017
KU748787.2, Shrew/DR|Crocidura leucodon−lab|SUI|~2010
MK644606.1, S95−1272|horse|SUI−GR|1995
OR468950.1, Z19_0095|human|GER−BY|2002
OR468949.1, Z19_0094|human|GER−BY|2002
100/100
95/96
100/100
100/95
100/100
95/88
100/99
100/96
100/100
100/100
0.004
4
3
2
1A
1B
5

1009

Figure 2. Phylogenetic analysis of complete coding BoDV-1 genome sequences. A Maximum likelihood tree (model SYM+G4) was calculated for all 90 complete coding BoDV-1 sequences (genome positions 54 to 8,822) of human and animal origin. Sequence BoDV-2 No/98 (AJ311524; not shown) was used to root the tree. Sequences generated during this study are depicted in bold. Statistical support is shown for major branches, using the format "SH-aLRT/ultrafast bootstrap". Clusters 2 to 5 and subclusters 1A and 1B are indicated by coloured branches and bars. Germany (GER): BB = Brandenburg, BY = Bavaria, BW = Baden-Wuerttemberg, NI = Lower Saxony, SH = Schleswig-Holstein, SN = Saxony, ST = Saxony-Anhalt; Switzerland (SUI): GR = Grisons; Austria (AUT): UA = Upper Austria.

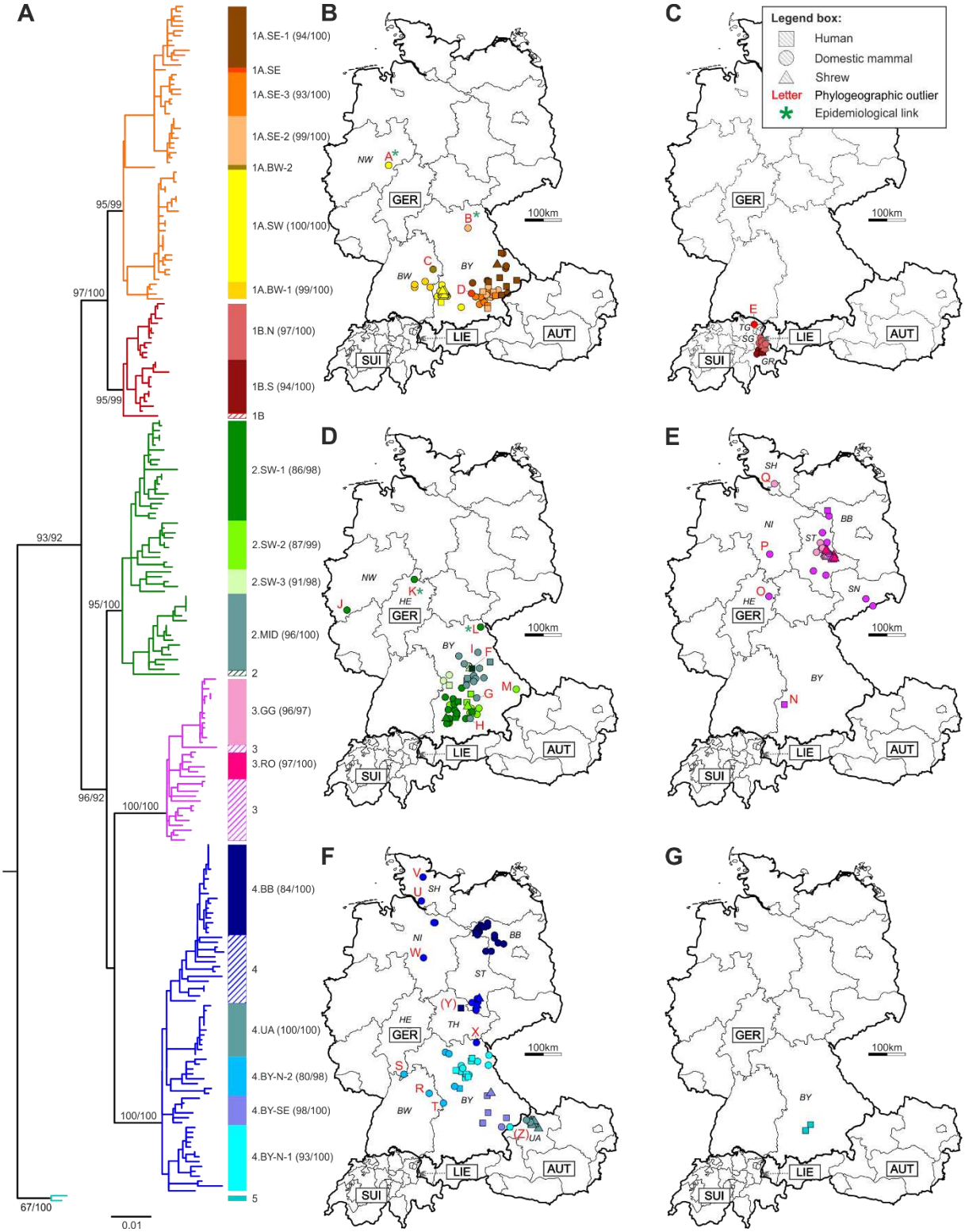

Figure 3. Detailed phylogeographic analysis of BoDV-1 clusters and subclusters. A) A Maximum likelihood (model GTR+F+I+G4) tree was calculated for 246 partial BoDV-1 sequences (1,824 nucleotides, nt) of human and animal origin that are covering the complete N, X and P genes (genome positions 54 to 1,877). Sequence BoDV-2 No/98 (AJ311524; not displayed) was used to root the tree. Statistical support is shown for main branches (including clusters, subclusters, and subclades), using the format "SH-aLRT/ultrafast bootstrap". Clusters 2 to 5 and subclusters 1A and 1B are indicated by coloured branches. Subclades are indicated by coloured bars and corresponding text labels, with statistical support of subclades shown in brackets. **B) to G)** Spatial distribution of subclusters 1A **(B)**

and 1B **(C)** and clusters 2 **(D)**, 3 **(E)**, 4 **(F)** and 5 **(G)**. Colours of the symbols represent the phylogenetic subclades indicated in panel A). Human sequences are generally mapped no more precise than to the centre of the district of the patient´s residence. Red letters represent phylogeographic outliers (see Extended Data Table 3). Green asterisks indicate known epidemiologic links into the dispersal area of the respective subclade. Germany (GER): BB = Brandenburg, BY = Bavaria, BW = Baden-Wuerttemberg, HE = Hesse, NI = Lower Saxony, NW = North Rhine-Westphalia, SH = Schleswig-Holstein, SN = Saxony, ST = Saxony-Anhalt, TH = Thuringia; Switzerland (SUI): GR = Grisons, SG = St. Gall, TG = Thurgau; Austria (AUT): UA = Upper Austria; Liechtenstein (LIE). Subclade designations: GG = Güterglück, MID = Middle, N = North, S = South, RO = Rosslau, SE = Southeast, SW = Southwest.

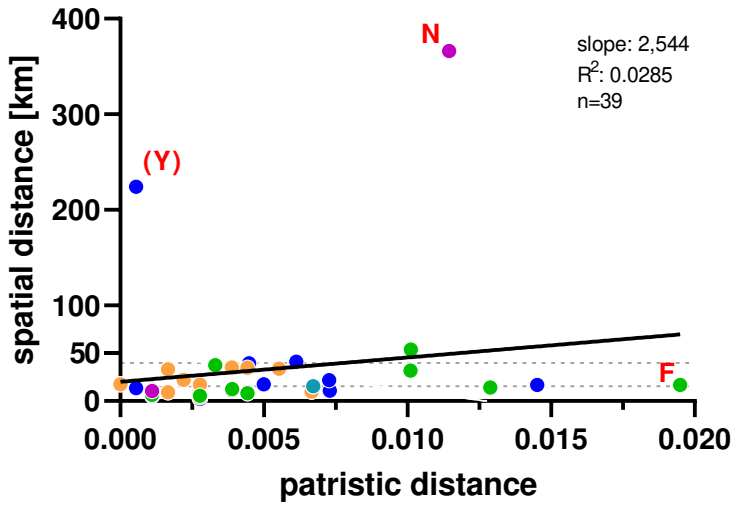

Figure 4. Geographic distance of human BoDV-1 sequences to their closest phylogenetic relatives. The minimal distance to the most closely related BoDV-1 nucleotide (nt) sequence was identified for all human BoDV-1 sequences with available geographic information (n=39) based on patristic distances calculated from the Maximum likelihood (ML) tree of 246 N-X/P nt sequences (Extended Data Figure 5). Sequences without available location as well as non-human sequences classified as phylogeographic outliers (Extended Data Table 3) were excluded from the analysis. For each human sequence, the minimal spatial distance was calculated to all sequences with a patristic distance of up to 1.2-fold the patristic distance to the phylogenetically closest relative. Colours of the dots represent phylogenetic clusters and subclusters as defined in Figure 2. Red capital letters indicate human cases identified as phylogeographic outliers (Extended Data Table 3). Sequence Z21_0139 (Y) is marked as a potential outlier due to its close genetic relation to animal sequences in more than 200 km distance. Broken horizontal lines represent the 90th percentile (39.8 km) and the median (15.6 km) of the dataset. The black line represents the linear regression of genetic and geographic distance. Slope and goodness of fit (R^2) of the regression line are provided.

Supplementary Files

This is a list of supplementary files associated with this preprint. Click to download.

- PhylogeographieBoDV1Supplementalsv7231117final.pdf